NASA CONTRACTOR REPORT

NASA CR-745

NASA CR-745

ANALYTICAL INVESTIGATIONS OF LAMINAR SEPARATIONS USING THE "CROCCO-LEES MIXING PARAMETER" METHOD

by D. R. Haworth and A. R. Peters

Prepared by

OKLAHOMA STATE UNIVERSITY

Stillwater, Okla.

for

NATIONAL AERONAUTICS AND SPACE ADMINISTRATION • WASHINGTON, D. C. • MAY 1967

29 NASA CR-745 END

3 ANALYTICAL INVESTIGATIONS OF LAMINAR SEPARATIONS USING THE "CROCCO-LEES MIXING PARAMETER" METHOD 6

By D. R. Haworth and A. R. Peters 8

26 29
Prepared under Grant No. NGR 37-002-028 by
OKLAHOMA STATE UNIVERSITY
Stillwater, Okla. 3

for

NATIONAL AERONAUTICS AND SPACE ADMINISTRATION

For sale by the Clearinghouse for Federal Scientific and Technical Information
Springfield, Virginia 22151 – CFSTI price $3.00

ABSTRACT

The design of advanced high-speed aircraft has prompted considerable interest in supersonic and hypersonic boundary layer separation problems. A review of the current analytical methods and available experimental data has been made for the two-dimensional flat plate-deflected flap configuration. The semi-empirical approach initially proposed by Crocco and Lees and as subsequently modified was used in the study. Improvements in the understanding of the mixing function correlation through the initial separation point and up to the plate-flap intersection have been presented. The necessity for coupling together the complete separated region from initial separation to final reattachment has been indicated.

TABLE OF CONTENTS

I. INTRODUCTION AND DESCRIPTION OF PROBLEM

The project objective is to explore in detail the laminar separated flow phenomenon, with emphasis on the separation region ahead of reattachment. This study program consists of analytical calculations supplemented by correlation with the available experimental data.

While the work contained in this report is principally concerned with the flow prior to reattachment, reattachment solutions have been studied with the aim of tying the entire interaction problem together. The reattachment and coupling techniques are discussed.

I-1. Justification of Interest

Current interest in "gliding type" re-entry bodies and recoverable booster stage rockets poses many design problems for the engineer and space scientist. Among the problems to be dealt with are control requirements and the prediction of pressures on the body surface. When the airflow separates from a surface, sudden and large changes frequently result in the aerodynamic pressure distributions. In the design of future hypersonic vehicles, separated flows and their effects on control characteristics must be well understood.

In the event that aerodynamic control surfaces are used, studies of the type presented will be helpful in assessing the size and responsiveness of these surfaces. Additionally, the analysis could be useful in determining the pressure distribution in the vicinity of two-dimensional compression corners which are structurally a part of the vehicle surface.

A re-entry vehicle enters the low density high altitude atmosphere at very high velocities. By a controlled descent, much of the orbital velocity can be dissipated prior to reaching the denser atmosphere where aerodynamic heating can be a significant problem. Flight such as this at supersonic and hypersonic speeds in low density air would be expected to promote the occurrence of laminar flow over much of the vehicle during the descent. High Mach numbers have a suppressing influence on the transition to turbulence, hence, laminar flow is more likely to occur at high Mach numbers.

I-2. Description of Physical Phenomena

Flow separation may be initiated by two broad classes of conditions. The first class, the one to be discussed, occurs when the flow advances against an adverse pressure gradient. This class is usually termed "boundary layer separation" as opposed to the "breakaway separation," the second class. Breakaway separations occur even though a favorable pressure gradient exists and are usually associated with flows past bluff bodies and sharp convex corners.

The principles underlying the two-dimensional boundary layer separation are now generally accepted. The boundary layer developed by a viscous fluid flowing over a body encounters skin friction effects at the wall and may additionally

encounter an upstream directed force. This latter force, in most fluid dynamic situations, results from the adverse pressure gradient. When these forces are such that the velocity gradient ($\partial u/\partial y$) at the wall becomes zero, the flow is on the verge of separating.

The so-called "free interaction" type of boundary layer separation is the classification which is of interest in this study. By "free interaction" we consider that the pressure distribution of the outer flow is the result of a mutual interaction between the boundary layer and the outer flow. In a free interaction the flow is independent of the direct influence of the downstream configuration and is also independent of the mode of inducing the separation. In a nonviscous flow field an impinging or generated shock wave will contact some point on the surface which is downstream from the leading edge. However, with viscous effects present, a developed boundary layer exists, and the shock wave does not reach the surface. The adverse pressure gradient may be generated by the shape of the body, as with a compression corner, or by an external source such as an impinging shock wave. In both cases, the flow experiences a pressure rise across the shock waves.

Figures 1 and 2 present the essential features of two types of free interaction separations. Both are for two-dimensional flows. The model in Figure 2 is the one principally used in this work, because most experimental studies have selected it. It should be mentioned that the separation and reattachment shocks coalesce into a single shock at a distance above the boundary layer. The fluid near the body passes through two weaker shocks, while the flow well out into the inviscid layer passes through only a single shock.

If the shock is of sufficient strength to cause separation, the external stream is deflected at the separation point, and "circulating" fluid is trapped below this streamline. This streamline, customarily referred to as the "dividing streamline," joins the body again at the reattachment point.

I-3. Design Applications

Considering the separation analysis from the perspective of the engineer who in the end must apply the theories in hardware applications, the problem becomes clouded with complications. The flow conditions ahead of the interaction and the geometry are the only quantities which the engineer knows in advance. The locations of separation and reattachment, and the distribution of pressures throughout the interaction region are not known initially. This is one important class of problems in which the static pressures are not given, but must be determined by the interaction between the "external" inviscid flow and the viscous layer near the surface.

The Crocco-Lees method is capable of embracing the entire separated interaction within a single framework once the semi-empirical features have been reasonably well accounted for. The problem can be analyzed by breaking the interaction region into three distinct parts. These parts include: 1.) flat plate Blasius type flow to separation, 2.) separation to plateau to shock impingement, and 3.) shock to reattachment to Blasius flat plate flow. By utilizing the empirical pressure plateau correlation and the downstream pressure ratio calculated

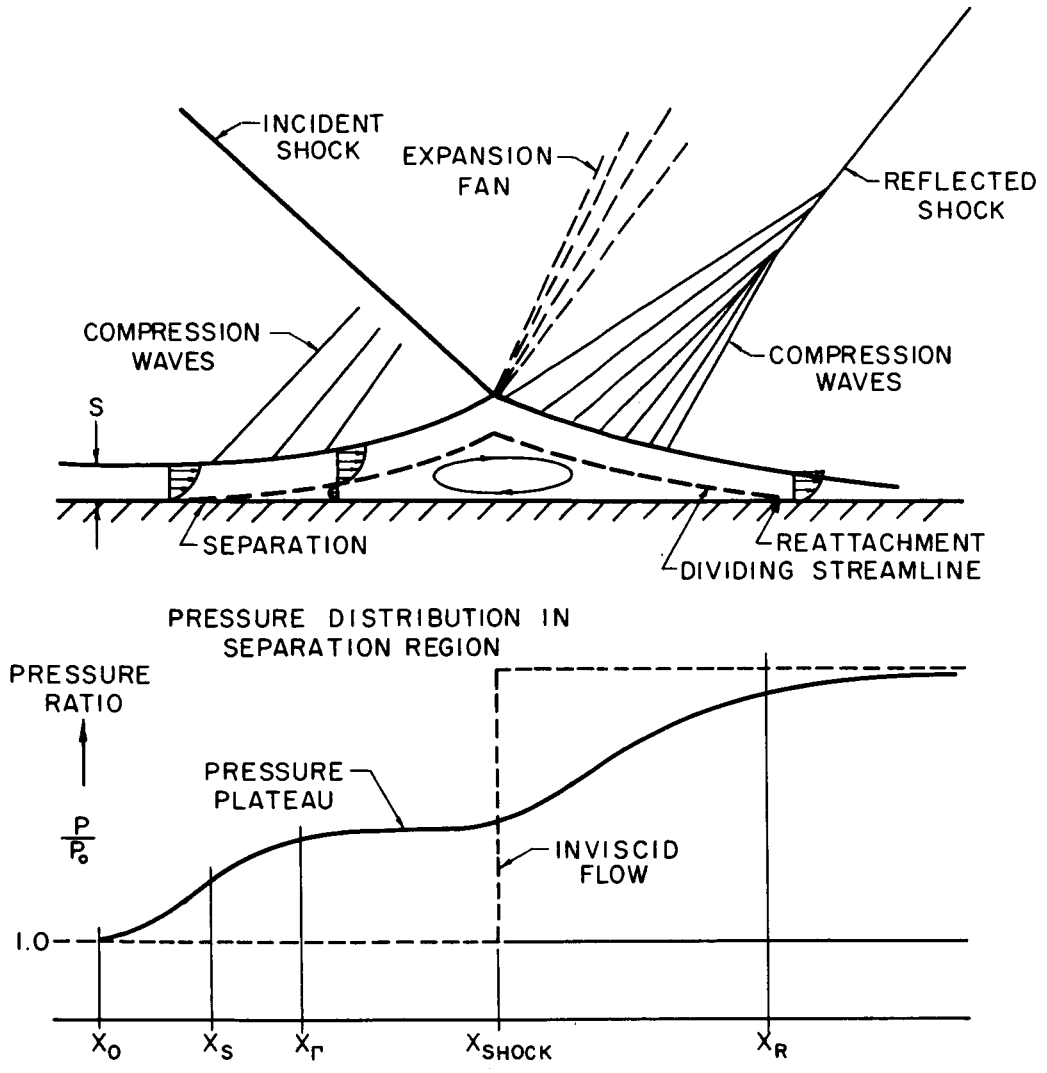

Figure 1. Shock Wave-Laminar Boundary Layer Interaction Model
Shock Generated by External Source

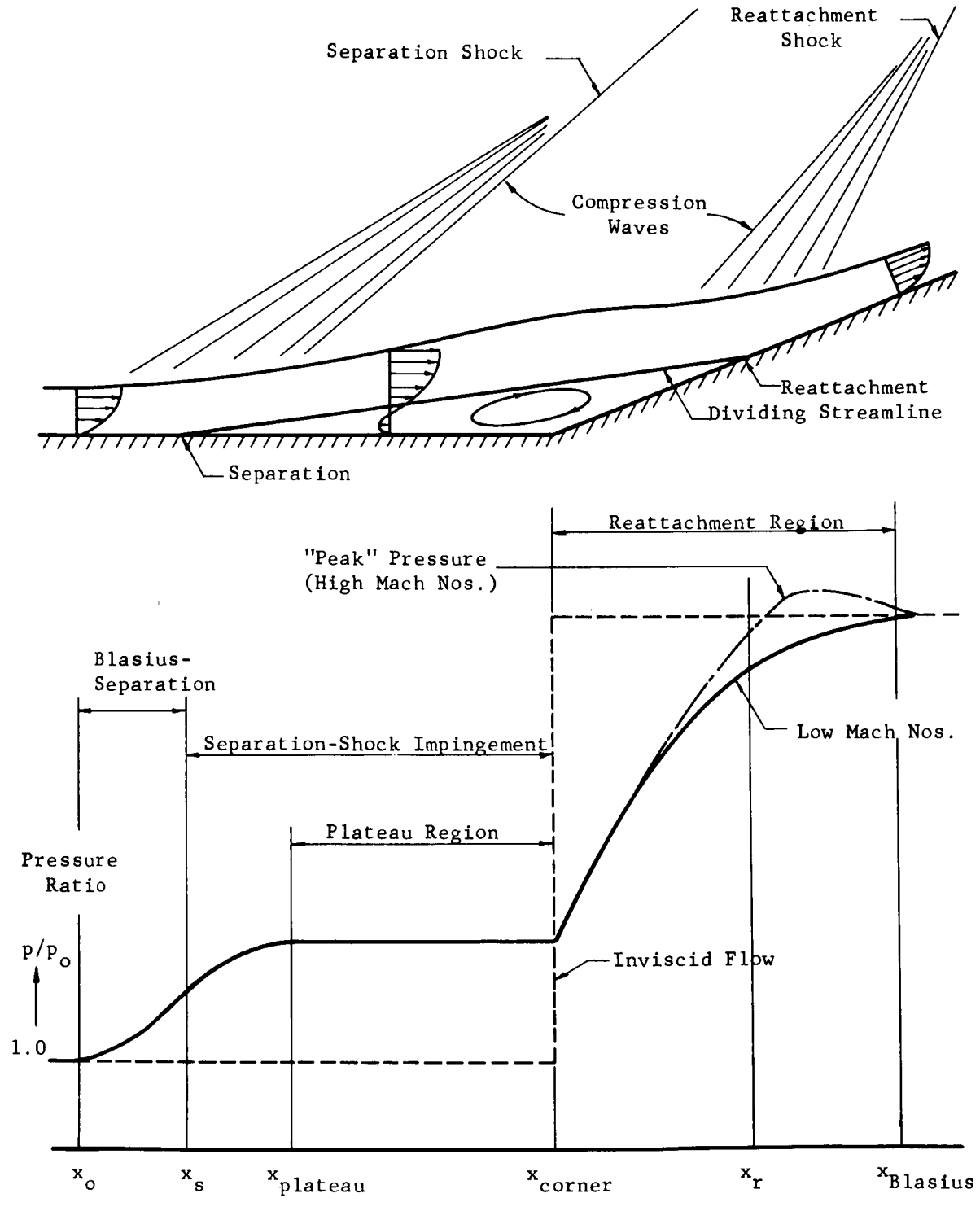

Figure 2. Shock Wave-Laminar Boundary Layer Interaction
Shock Generated by Ramp

from inviscid theory, it is hoped to tie the three segments together. A straight dividing streamline which connects the separation and reattachment points will be assumed. To approximate the breakaway angle which this streamline makes with the plate, the inviscid turning angle dictated by the empirical plateau pressure will be used. By first "guessing" a separation point, the reattachment point becomes fixed. It should be mentioned that the physical conditions at reattachment are not well known at present. The pressure ratio at the reattachment point is not known, however, in general it would be expected that it would be lower than the final downstream value. By working the solution through to the shock, and then matching pressure ratios across the shock, it will be determined if sufficient mixing has occured in the plateau region to accomplish reattachment at the known higher pressure downstream.

If the length of the mixing region (pressure plateau) is too short to accomplish the inviscid reattachment pressure rise, a new separation location further forward on the plate will be selected. Iteration will produce the optimum location for the separation point, and hence, will give the pressure distribution throughout the entire interaction. This technique is of no value in explaining unknowns in the reattachment phenomenon, but, it does provide a mechanism for linking the regions together.

I-4. Why the Crocco-Lees Method Was Selected

In considering the foundation upon which to base the separation development, the design engineer was kept uppermost in mind. Simplicity of use, conceptual understanding, and accuracy were the prime considerations given.

The Crocco-Lees method gives a qualitative interpretation of the velocity profile characteristics by making use of the velocity profile parameter, K. Different K's are associated with different velocity profiles. This gives a conceptual feeling for the changes which occur without becoming involved in the mathematics which describe the actual profile shape. This method is consistent with the concept that the velocity profile is dependent upon its previous "history." This is born out by the fact that K at separation differs from K at reattachment--as would be expected because of the different "histories" is each case.

The principal shortcoming of the method is that the semi-empirical parameters which appear in the development must be determined on the basis of experimental results. A corresponding disadvantage of purely analytical solutions is that they require the selection of velocity profiles to describe the flow. This becomes a very involved process because non-similar profiles are needed to describe the physical behavior throughout the pressure plateau region. Another consideration is that a semi-empirical technique should lend itself to extensions, paricularly in the case of the turbulent boundary layer.

II. ANALYTICAL INVESTIGATION

II-1. Background of Previous Investigations

Considerable material has been presented in the open literature pertaining to the laminar separation problem. The discussions in this section and Appendix A will be brief--referral to the references will be needed to complete many of the details.

The major portion of this section will be devoted to a discussion of the Crocco-Lees method and the modifications which resulted principally from Glick's work. The Lees and Reeves method will be discussed briefly because of its current popularity. Four other popular techniques are described in Appendix A.

II-1-1. Crocco-Lees Method. The original Crocco-Lees paper which appeared in 1952 (1)* dealt with flows up to the point of separation for compression corners and for the aft flow over a supersonic airfoil with a blunt training-edge. The original concepts which apply up to the point of separation have remained basically unchanged except for the behavior of the empirical parameter C(K). Glick (2) has extended the technique to include the separated region and cleared up some troublesome details near separation--such as the correct behavior of C(K).

This method, like nearly all analytic solutions which have been proposed in the literature, makes use of the integral momentum technique as a means of simplifying and handling the boundary layer equations. The boundary layer profiles are absorbed in the definition of a new velocity profile parameter.

The Crocco-Lees method is based upon the assumption that the parameters describing the boundary layer are dependent upon the rate of entrainment of fluid into the boundary layer from the external stream and that there exist certain universal correlation functions which relate these parameters. The analytical development for the method hinges on the velocity profile shape parameter, K, which is defined as the ratio of the momentum flux to the product of mass flux and local external velocity. It is expressed as

$$K = \frac{I}{\bar{m} u_e} = \frac{\text{momentum flux}}{\text{mass flux} \times u_e} \tag{1}$$

where

$$I = \int_0^\delta \rho u^2 dy$$

$$\bar{m} = \int_0^\delta \rho u \, dy \ .$$

---

*Numbers in brackets refer to references at the end of this report.

This basic parameter, which characterizes the flow in the viscous region, can be shown (1,2) to be defined in terms of either compressible or incompressible boundary layer variables as

$$K = \frac{\delta - \delta^* - \delta^{**}}{\delta - \delta^*} = \frac{\delta_i - \delta_i^* - \delta_i^{**}}{\delta_i - \delta_i^*} \quad . \tag{2}$$

The Stewartson (3) transformation, which assumes a Prandtl number of unity and viscosity proportional to the absolute temperature, is utilized to transform a compressible boundary layer.

By dividing the momentum flux by the mass flux, a mean velocity (u_1) for the viscous region is obtained. Also, without attaching any significance to the definition, one can think of a mean-temperature (T_1) across the viscous region. Crocco-Lees develops a parameter, called f, which describes the mean temperature-mean velocity relationship. This parameter is found in terms of the boundary layer variables to be

$$f = \frac{\left(\delta_i - \delta_i^* - \delta_i^{**}\right)\delta_i}{\left(\delta_i - \delta_i^*\right)^2} = \frac{K\,\delta_i}{\left(\delta_i - \delta_i^*\right)} \quad . \tag{3}$$

In a sense, the deviations of f and K from unity measure the nonuniformity of the velocity profile. For every incompressible boundary layer flow, f and K can be related to each other. Compressible boundary layers may be expressed in an equivalent incompressible form. Once transformed, each point in the flow region corresponds to a point in the f-K plane, and the whole class of flows (attached, separating, separated, etc.) is represented by a single locus of points in the f-K plane.

For purposes of analysis, the flow is divided into two parts--an outer region which is assumed to be essentially nondissipative, and an inner region in which the viscosity is assumed to play an important role. Figure 3 expresses the separated region in terms of Crocco-Lees' language. The extent of the viscous region is measured by the length, δ, which for the case of a body in high-Reynolds-number stream is the usual boundary layer thickness. The definition of the length δ is artificial, and physical quantities such as pressure and interaction distance are not sensitive to the definition of δ. To develop and handle the equations describing the flow, the chief assumptions are:

1. Gradients of viscous stresses are negligible compared with the static pressure gradient in the flow direction
2. Zero pressure gradient normal to surface
3. Steady flow
4. The external flow over the adiabatic wall is supersonic and isentropic. The flow direction at $y=\delta$ is given by the Prandtl-Meyer relation.
5. Prandtl number of one
6. Viscosity proportional to the absolute temperature
7. Flow angles relative to the wall are small
8. Gas is thermally and calorically perfect
9. Constant stagnation temperature throughout the whole region
10. Laminar viscous region

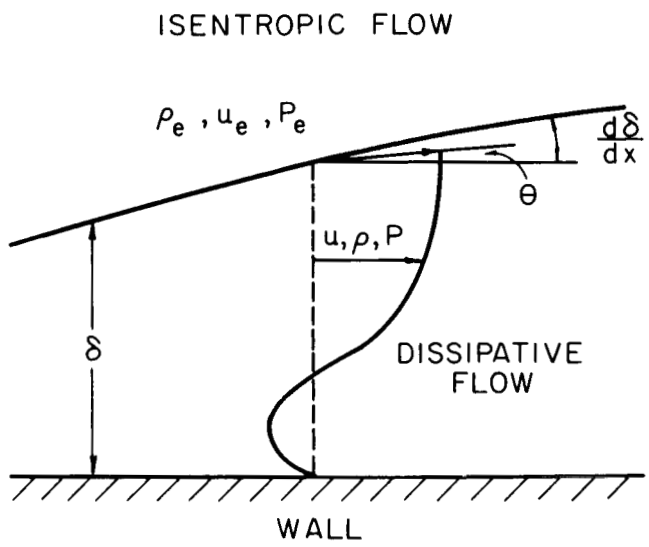

Figure 3. Flow Regions as Described by Crocco-Lees

The flow within the viscous region is described by the momentum and continuity equations which can be obtained in the following forms (2):

$$\frac{d}{dx}(mKw_e) = w_e\left(\frac{dm}{dx}\right) - \frac{Pw_e c_f}{2\Phi_e} - \delta\left(\frac{dp}{dx}\right) \tag{4}$$

$$\frac{dm}{dx} = \left(\frac{P}{\Phi_e}\right)\left(\frac{d\delta}{dx} - \theta\right) \tag{5}$$

where $\Phi_e = \frac{(1 - \frac{\gamma-1}{2} w_e^2)}{\gamma w_e}$, $w_e = u_e/a_t$, and θ is the direction of the streamline at the edge of the boundary layer. The external inviscid insentropic flow is described by the Bernoulli equation

$$\frac{dp}{p} = \left(\frac{-dw_e}{\Phi_e}\right). \tag{6}$$

In addition, one has the mean temperature equation $m = P\delta/\Phi_1$ and the Prandtl-Meyer relationship $\theta = \theta(w_e)$. From this system of equations, p and θ are eliminated, leaving three equations and six unknowns (δ, m, K, w_e, c_f, and Φ_1). To account for the three remaining unknowns and thus complete the mathematical formulation of the method, semi-empirical coefficients are introduced. These account for the mean temperature, the skin friction, and the mixing in the viscous region. These additional parameters, all dependent on K, are defined as F(K), D(K), and C(K). F(K) is related to the mean temperature-mean velocity correlation, D(K) is the skin friction correlation function, and C(K) is the mixing rate correlation function. These are expressed as follows:

$$F = F(K)$$

$$c_f = D(K)\,\mu_e a_t/m$$

$$k = (d\delta/dx - \theta) = C(K)\,\frac{\mu_e a_t}{m}\,.$$

F and f are related by

$$F = \left(\frac{f}{K^2}\right) - 1 = \frac{\delta_i^* - \delta_i^{**}}{\delta_i - \delta_i^* - \delta_i^{**}}\,. \tag{7}$$

The functional dependence of these empirical coefficients must be obtained through correlation with experiments--in hope of predicting the "universal" behavior for each.

By using these definitions of C(K), F(K), and D(K) in the original three equations, they may be solved simultaneously to obtain the following set of non-linear first order differential equations:

(8)

$$\frac{dk}{d\zeta} = \frac{-KF}{c} \frac{\left\{ \frac{c}{\zeta} \left[t - K(F+t) - \frac{(1-K)(1-\sigma)}{KF} \left(K(F+t)(1-\frac{3\gamma-1}{2} M_e^2 t) + KM_e^2 t^2(\gamma-1)\right)\right] + \theta \right\}}{\left\{ K(F+t)(1-\frac{3\gamma-1}{2} M_e^2 t) + K(\gamma-1) M_e^2 t^2 - KF(F+t+K\frac{dF}{dK}) \right\}}$$

(9)

$$\frac{dM_e}{d\zeta} = \frac{-M_e}{C} \frac{\left\{ \frac{c}{\zeta} \left[t - K(F+t) - (1-\sigma)(1-K)(F+t+K\frac{dF}{dK}) \right] + \theta \right\}}{\left\{ K(F+t)(1-\frac{3\gamma-1}{2} M_e^2 t) + (\gamma-1) KM_e^2 t^2 - KF(F+t+K\frac{dF}{dK}) \right\}} .$$

These two general equations may be specialized to the various flow regions by the proper selection of the parameters C(K), D(K), and F(K).

Blasius-Separation

In the region upstream of separation the boundary layer is attached. In the original Crocco-Lees paper, the Falkner-Skan profiles were used to predict C(K) and D(K) in this region and F(K) was determined by a maximation principle. Glick established that the C(K) given by the Falkner-Skan solution was incorrect and improved upon this by using experimental and analytical solutions for the Schubauer ellipse. By using the following approximations,

$$F(K) = \frac{2(1-K)}{(2k-1)}$$

$$D(K) = 22.2\ (K - .630)$$

$$C(K) = 36.2\ (K - .630)$$

equations (8) and (9) are then linearized with respect to Mach number to give

$$\frac{dK}{d\zeta} = -L \left[\frac{P}{\zeta} - \epsilon \right] \tag{10}$$

$$\frac{d\epsilon}{d\zeta} = -N \left[\frac{Q}{\zeta} - \epsilon \right] . \tag{11}$$

It is assumed that $M_e = M_\infty + \epsilon$, where $\epsilon << M_\infty$ and θ is given by the linearized Prandtl-Meyer relationship

$$\theta = \frac{-\sqrt{M_\infty^2 - 1}\ \epsilon}{M_\infty (1 + \frac{\gamma - 1}{2} M_\infty^2)}$$

The ζ term is likened to the Reynolds number because of its behavior. The quantities L,N,P, and Q are all functions of K and are given by:

$$L = \frac{2K(1-K)(2K-1)^2\sqrt{M_\infty^2-1}}{4M_\infty K(1-K)(2K^2-2K+1)(1+\frac{\gamma-1}{2}M_\infty^2)\,C(K)S}$$

where

$$S = \left[1 - \frac{\gamma M_\infty (2K-1)^2}{2(2K^2-2K+1)(1+\frac{\gamma-1}{2}M_\infty^2)} - \frac{(2K-1)^3(M_\infty-1)}{4(2K^2-2K+1)(1-K)(1+\frac{\gamma-1}{2}M_\infty^2)^2}\right],$$

$$N = \frac{LM_\infty}{KF(K)} = \frac{LM_\infty(2K-1)}{2K(1-K)},$$

$$P = \frac{C(K)M_\infty}{\sqrt{M_\infty^2-1}}\left[\sigma(1-K) + \frac{(2K+1)(1-\sigma)}{2K}\left\{\frac{2\gamma K(1-K)M_\infty^2}{(2K-1)} + K\left(\frac{\gamma+1}{2}\frac{M_\infty^2}{(1+\frac{\gamma-1}{2}M_\infty^2)} - 1\right)\right\} - \frac{2K(1-K)(1+\frac{\gamma-1}{2}M_\infty^2)}{(2K-1)}\right],$$

$$Q = \frac{C(K)M_\infty}{\sqrt{M_\infty^2-1}}\left[\sigma(1-K) - \frac{2(1-K)K(1+\frac{\gamma-1}{2}M_\infty^2)}{(2K-1)}\left\{1 - \frac{(1-\sigma)(2K^2-2K+1)}{K(2K-1)}\right\}\right],$$

$$\sigma = D(K)/2(1-K)\,C(K).$$

Separation to Shock Impingement

Beyond the separation point the flow is detached. It is assumed that the skin friction at the wall is sufficiently reduced so that it can be neglected in this region. As a first approximation, F(K) is taken as constant, equal to the separation value. The mixing correlation function, C(K) is more elusive and must follow a trajectory such that the correct pressure distribution results. This behavior will be discussed in more detail in Section III. By taking

$$D(K) = 0$$

$$F(K) = F_{sep} = F_s$$

$$C(K) = C$$

the generalized equations, when linearized become

$$\frac{dK}{d\zeta} = \frac{-F_s\sqrt{M_\infty^2-1}}{M_\infty(1+\frac{\gamma-1}{2}M_\infty^2)Cb}\left[\frac{CM_\infty(1+\frac{\gamma-1}{2}M_\infty^2)}{\sqrt{M_\infty^2-1}\,\zeta}\left(\frac{F_s^2-(1-K)b}{F_s}\right)+\epsilon\right], \qquad (12)$$

$$\frac{d\epsilon}{d\zeta} = \frac{-\sqrt{M_\infty^2-1}}{K(1+\frac{\gamma-1}{2}M_\infty^2)Cb}\left[\frac{CM_\infty(1+\frac{\gamma-1}{2}M_\infty^2)F_s}{\sqrt{M_\infty^2-1}\,\zeta}+\epsilon\right], \tag{13}$$

where

$$b = F_s^2+\frac{\gamma F_s M_\infty^2}{(1+\frac{\gamma-1}{2}M_\infty^2)}+\frac{(M_\infty^2-1)}{(1+\frac{\gamma-1}{2}M_\infty^2)}.$$

Mixing in this region is of paramount importance. After separation the flow is essentially divided into two parts by the dividing streamline. The fluid along the dividing streamline is accelerated by viscous momentum transfer in the region between separation and the beginning of reattachment and is thereby prepared for the forthcoming reattachment pressure rise when fluid along the dividing streamline is stagnated.

For the entire region between the Blasius point and shock impingement, transformation back to the real plane is made by using

$$\frac{X_s - X}{X_s} = \frac{1}{Re_{X_s}}(1+\frac{\gamma-1}{2}M_\infty^2)^2\int_\zeta^{\zeta_s}\frac{\zeta d\zeta}{C(K)}\frac{M_\infty}{M_e}\left[\frac{1+\frac{\gamma-1}{2}M_e^2}{1+\frac{\gamma-1}{2}M_\infty^2}\right]^{\frac{3\gamma-1}{2(\gamma-1)}} \tag{14}$$

where

$$Re_{X_s} = \frac{\rho_\infty U_\infty X_s}{\mu_\infty}.$$

Reattachment

The reattachment solution differs in that the generalized equations (8) and (9) are not adapted to this region. Instead, the momentum equation (4) is reduced to

$$dK = (1-K)\left(\frac{dm}{m}\right) + KF\left(\frac{dM_e}{M_e}\right) \tag{15}$$

by neglecting the skin friction at the wall. The experiments by Chapman, et. al. (4), justify the belief that during reattachment the viscous effects are not important. By neglecting the mixing (C(K) = 0), one obtains

$$k = 0 = \left(\frac{d\zeta}{dx}\right) - \theta$$

which can be written

$$dx = \frac{d\delta}{\theta} \quad .$$

By non-dimensionalizing and integrating,

$$\frac{x}{x_{sh}} = 1 + \int_{\frac{\delta_{sh}}{x_{sh}}}^{\frac{\delta}{x_{sh}}} \frac{d\left(\delta/x_{sh}\right)}{\theta} \tag{16}$$

results. The explicit integration of this equation determining x is carried out by assuming that the F(K) relation joining the shock and the Blasius point is linear. C(K) and D(K) have both been neglected as being negligibly small.

Matching of Conditions at Blasius Point

Since the method of solution requires the matching of conditions at the upstream Blasius point, ε and ζ must be known at this location. These values are obtained by assuming that a weak hypersonic interaction exists and then solving to find ε_b and ζ_b. These are given by the following two equations:

$$\zeta_b = \left(t\sqrt{.44Re_x}\right)\Big/(1-K) \tag{17}$$

$$\varepsilon_b = \frac{M_\infty \left(1 + \frac{\gamma-1}{2} M_\infty^2\right) C(K)(1-K)^2}{\sqrt{M_\infty^2-1}\ \sqrt{.44Re_x}} \left(1 - \frac{KF}{(1-K)} \left(1 + \frac{\gamma-1}{2} M_\infty^2\right)\right)\Bigg|_{K = K_b} \tag{18}$$

where

$$Re_x = \frac{\rho_\infty u_\infty x_b}{\mu_\infty} \quad .$$

A weak hypersonic interaction imposes the limitation that the leading edge must be sharp. If the Reynolds number, based upon the leading edge radius, has a value of less than one hundred, the interaction is generally assumed to be weak.

II-1-2. Lees and Reeves Method. The main attempt of the Lees and Reeves (5) method was to develop a theory which is capable of including the entire separated flow within a single framework, without introducing semi-empirical features. To describe this flow approximately, including the subsequent reattachment, an integral or moment method is used in which the first moment of the momentum is employed, in addition to the usual (zeroth moment) momentum integral.

The velocity and enthalpy profiles are characterized by a single independent parameter, a , not explicity related to the local static pressure gradient. The successful application of this method to separated and reattaching flows hinges on the proper choice of the one parameter family of velocity profiles utilized to represent the integral properties of the viscous flow. The Stewartson (6) reversed-flow profiles were found to have the quantitatively correct behavior while polynomials did not. For flows with heat transfer, the Cohen-Reshotko (7) profiles are used.

The Lees and Reeves method employs the same assumptions that were used by Crocco-Lees. The desired form of the equations is obtained by first transforming the compressible boundary layer equations into an equivalent incompressible form by making use of the Stewartson (3) transformation.

Once in incompressible form, the momentum integral is obtained by integrating the "equivalent" incompressible boundary layer momentum equation across the boundary layer. In a similar manner, the first moment of momentum can be obtained by multiplying the momentum equation by u_i and integrating across the boundary layer. These two equations in conjunction with the boundary layer continuity equation describe the viscous region.

The external inviscid flow is not a known quantity but must be determined by the normal velocity induced by the growth of the boundary layer. The inclination of the streamline in the external inviscid flow at $y = \delta$ is given by the Prandtl-Meyer relationship. This relationship is then transformed to equivalent incompressible flow by using the Stewartson transformations.

Because the compression waves generated by the growth of the boundary layer coalesce into a shock wave well beyond the outer edge of the boundary layer, the isentropic Prandtl-Meyer relationship between M_e and θ is a good approximation at the edge of the boundary layer. The linearized Prandtl-Meyer relation,

$$\theta = \frac{-\sqrt{M_\infty^2 - 1}\ \epsilon}{\left(1 + \frac{\gamma-1}{2} M_\infty^2\right) M_\infty} , \tag{19}$$

where $M_e = M_\infty + \epsilon$, may be used when the supersonic-hypersonic similarity parameter $\sqrt{M_e^2-1}\ \tan\theta$ is small compared with unity, and $\tan\theta \backsimeq \theta$.

The linearized Prandtl-Meyer equation (19) together with the transformed Prandtl-Meyer relationship describe the inviscid region. By simultaneously solving the viscous and inviscid equations, and by making use of newly defined functions, the following two equations, convenient for numerical integration are obtained:

$$\left(\delta_{t/M_e}^{*\prime} \right) \frac{dM_e}{d\delta_t^*} = \frac{N_1}{N_3} \tag{20}$$

and

$$\delta_t^* \left(\frac{da}{d\delta_t^*} \right) = \frac{N_2}{N_3} \left[\frac{1}{\left(\frac{dH}{da} \right)} \right] . \tag{21}$$

N_1, N_2, N_3, and dH/da are all functions dependent upon a , which in turn depends on the profile family selected.

The dependent variables in (20) and (21) are ε (or M_e) and δ_t^* compared with ε and ζ in the Glick method. The mechanics for solution in both techniques are similar. The variables at the separation point must be repeatedly guessed in hopes of arriving at the correct Blasius point values. Once the Blasius to separation region has been solved, the solution downstream from separation follows in a straightforward manner, just as in the Crocco-Lees method.

Methods discussed in References 8-13 are briefly described in Appendix A.

II-2. Limitations of Analytical Methods

This section discusses the inherent limitations of the two methods discussed in Section II-1. Both techniques utilize the same boundary layer assumptions and are applicable only to two-dimensional geometries. Limitations pertaining to both as well as those affecting each method individually are discussed.

II-2-1. Both Crocco-Lees and Lees and Reeves. Both methods make the assumption that $\varepsilon << M_\infty$ where $M_e = M_\infty + \varepsilon$. As the Mach number increases, the assumption becomes more subject to question. At Mach 2.0, ε_b may be on the order of .01 of M_{e_b}, while for the same Reynolds number at Mach 7, ε_b is about .1 of M_{e_b}. Continuing to higher Mach numbers--at Mach 10, ε_b is about .3 of M_{e_b}, which certainly would result in invalidation of the assumption.

Figure 4 shows how the absolute value of the ratio of ε_b/M_∞ varies as a function of Mach and Reynolds numbers. ε_b was calculated using equation (18) and also by using a linearized form in which $M_\infty > 1$. It is noted that the linearized and exact relations approach one another at higher Mach numbers, and that the ε_b/M_∞ ratio increases with Mach number. Figure 4 illustrates only the relationship at the Blasius point. The linearization assumption becomes subject to even greater errors downstream from the Blasius point.

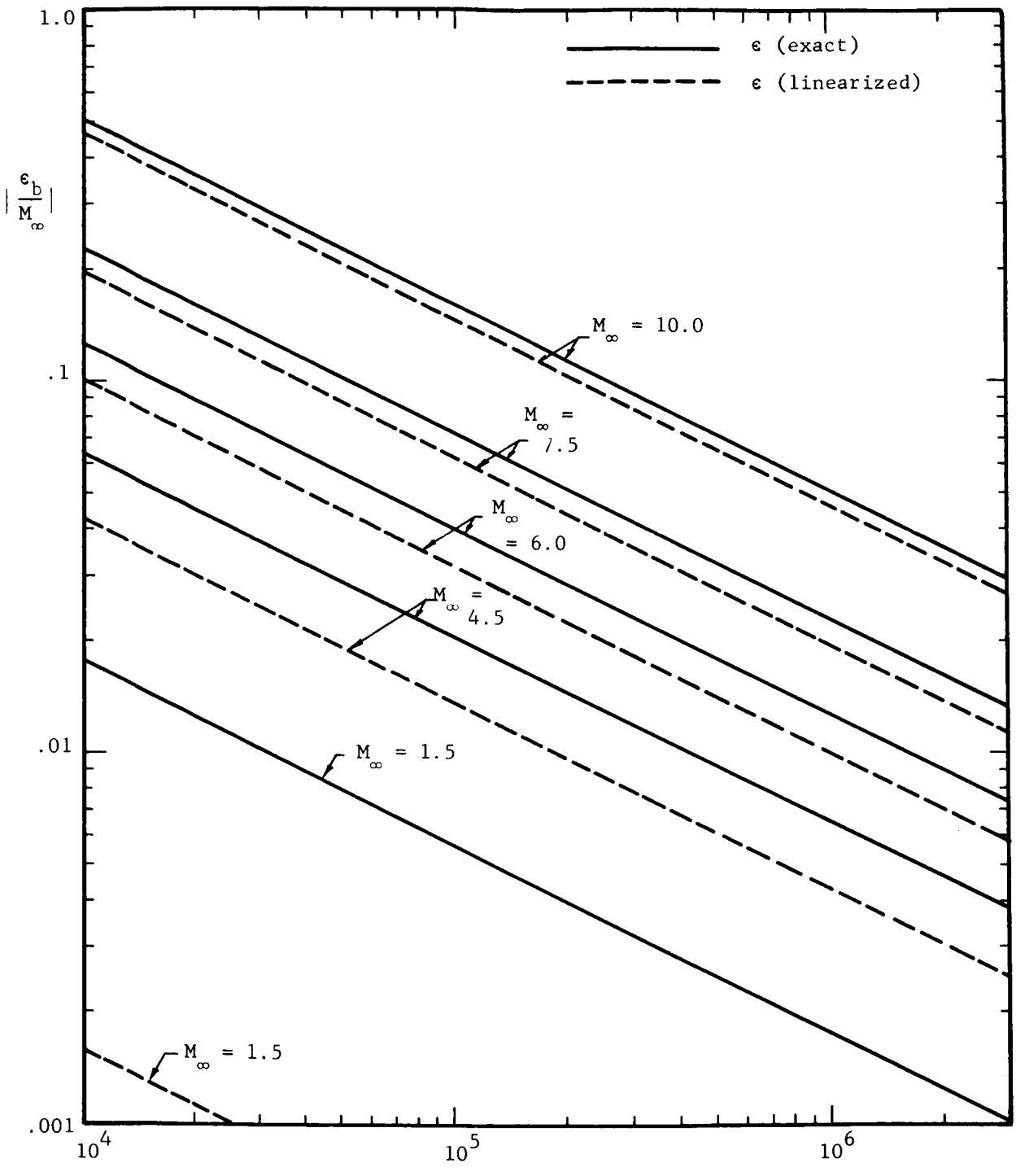

Figure 4. $\left|\frac{\epsilon_b}{M_\infty}\right|$ as a Function of M_∞ and Re_b

II-2-2. Crocco-Lees. As brought out in the previous discussions, the principal limitation in the Crocco-Lees method is the proper selection of the functions which describe F(K), D(K), and C(K). This may be overcome as more data becomes available. The results in Part III represent a first attempt at generalizing the C(K) function in the separation to shock impingement region.

II-2-3. Lees and Reeves. The Lees and Reeves method is dependent upon finding a correct one-parameter family of velocity profiles. The profile parameter, a, which is the dependent variable has a trajectory through the separation interaction as shown in Figure 5. The attached portions of the boundary layer (prior to separation and after reattachment) are described by one set of coefficients in which "a" varies between 0 and 1.58. In the separated region, another set of coefficients is used, and, in this case, "a" can take on values between 0 and 1. The maximum value of "a" is dependent upon the strength of the shock. The stronger the shock, the higher the value of "a" obtained. The problem arises in that for adiabatic separated flows, the profiles have been solved only in the range $0<a<.54$. For stronger interactions, an equivalent Falkner-Skan family of profiles must be solved to evaluate the profiles for "a" greater than .54.

In applying the Lees and Reeves method, Gulbran et al (14) noted that they were unable to calculate the reattachment for the high final pressures produced by 15^{o} and $22\frac{1}{2}^{o}$ ramps at Mach 8.

II-3. Difficulties and Problem Areas in Crocco-Lees Method

II-3-1. Blasius - Separation. The greatest difficulty in this region appears to be obtaining the desired slope for the pressure distribution. Also, the curve is approximately straight in many cases and has little curvature at the Blasius point transition. In general, the calculations yield reasonable pressure ratios at the separation point despite the way the pressure is distributed in this region.

The linear approximation for C(K) versus K may not be the optimum one in this region. Since very few experimental pressure measurements describe the regions immediately adjacent to the separation point, further refinements in C(K) do not seem to be justified at present for this region. A far more serious problem in this region results from the interaction induced by the leading edge of the plate. At lower Mach numbers this may not be significant, but, at higher values the results become appreciable.

II-3-2. Separation to Shock Impingement. Glick (2) proposes two techniques for treating the C(K) values in the region between separation and the shock. He conjectures that C(K) rises from zero at the separation value of K to some maximum value at the beginning of the plateau and that C(K) remains constant until the shock impingement is reached. As an approximation for this distribution of C(K), Glick offers a "simplified" and "refined" approach. In the simplified case, C(K) takes on a constant value $\bar{C}$ throughout the whole region. In the refined case, C(K) has a value of C_1 between separation and the plateau and a value of C_2 throughout the plateau region. These C(K) curves are illustrated in Figure 6.

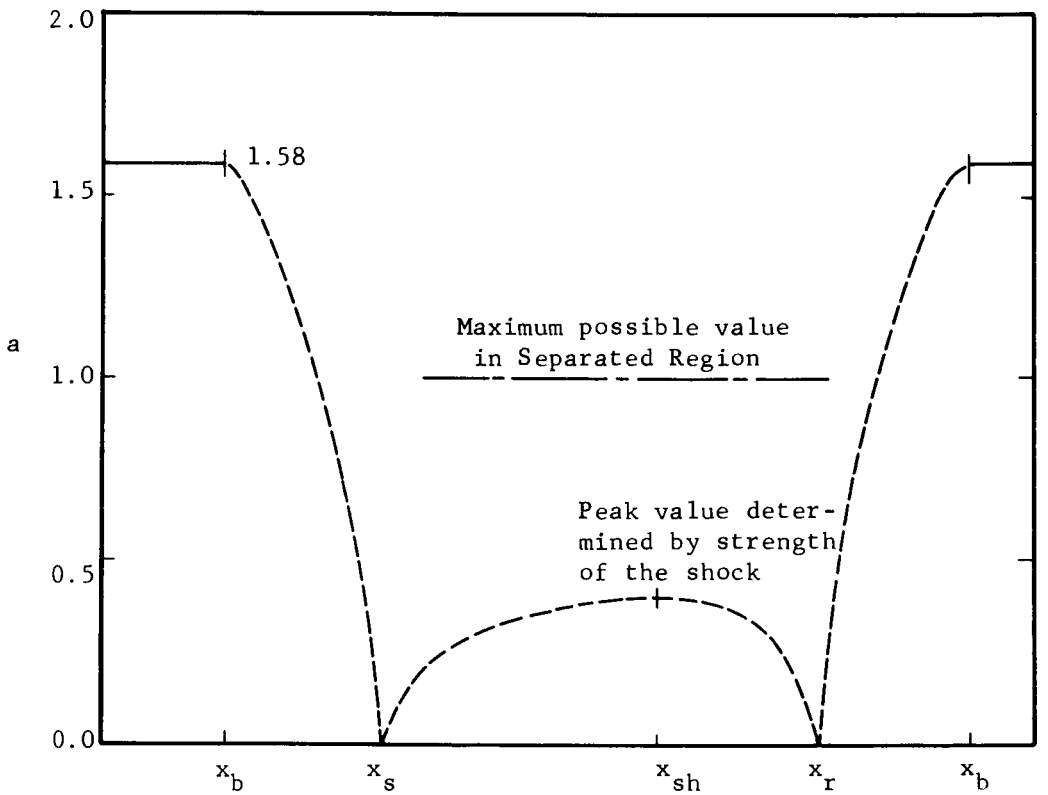

Figure 5. Characteristics of Lees and Reeves Velocity Profile Parameter in the Interaction

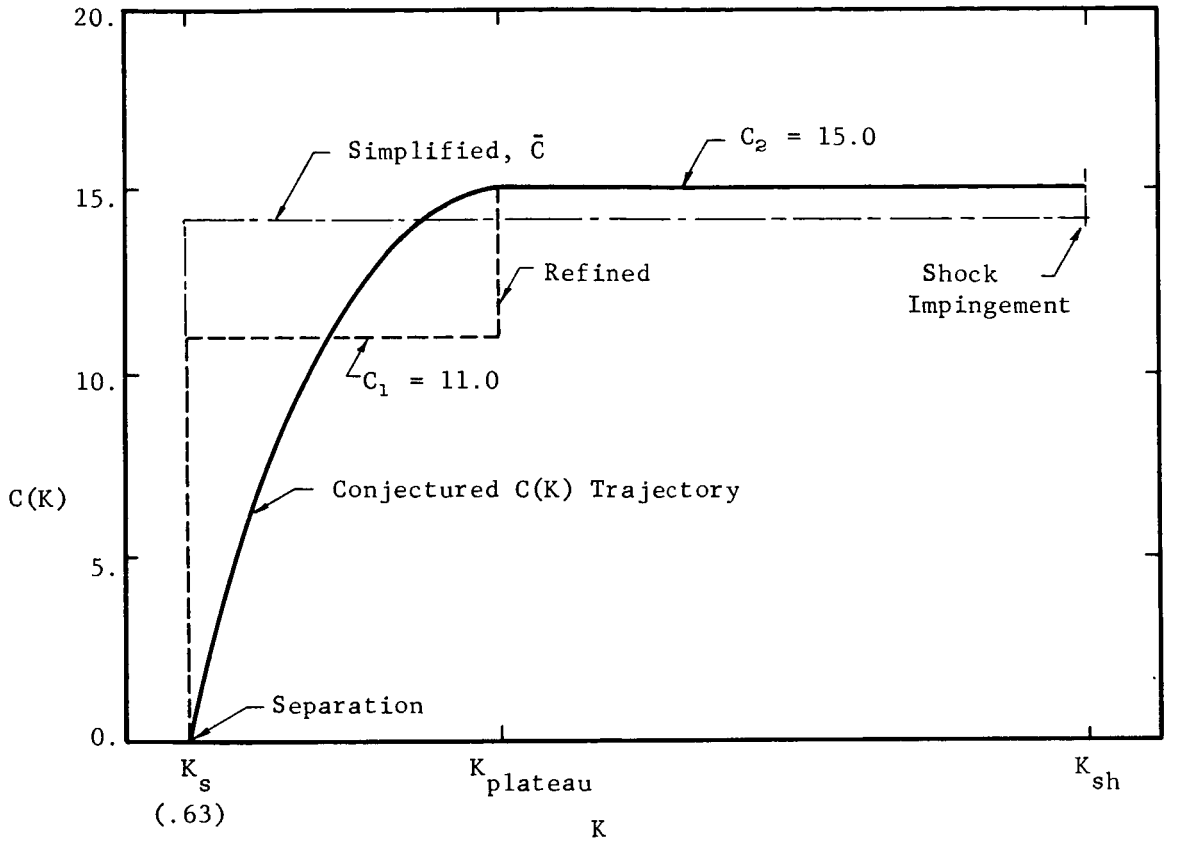

Figure 6. Glick's C(K) Trajectories Between Separation and Shock Impingement

The values of $C_1 = 11.0$ and $C_2 = 15.0$ were presented by Glick and were obtained from one set of experimental data (Mach 2.45). These values were suggested as "universal" for all separations. The results of this study indicate that C(K) takes on a behavior different from that specified by Glick. In the first place, C_1 does not universally equal 11.0 but appears to have a dependency on Mach number and possibly on the Reynolds number at the beginning of the interaction. A constant value of C_2 in the plateau region was found to produce a decreasing pressuure ratio rather than the constant value which is known to exist. If a constant pressure ratio is to be maintained, the C(K) parameter must continually increase with increasing K in the plateau.

II-3-3. Reattachment. The reattachment region has caused considerable difficulty--particularly in getting a pressure distribution which has the qualitatively correct behavior. At the present time it is felt that additional considerations must be given to this treatment before much reliance can be placed in the method. The calculation difficulties in this region are discussed in Part III.

A problem which will need to be accounted for in this region is the "peak pressure" which occurs after reattachment--before returning to the value of the inviscid downstream pressure rise. A pressure overshoot or "peak" is experienced because the flow near the surface passes through two weaker shocks, while the flow further out in the free stream crosses only a single, but stronger, shock system. The double compression by the flow near the surface produces a greater pressure rise than does the single compression. This peak pressure was not observed on low Mach number experimental data, while at moderate and high Mach numbers the overshoot becomes quite noticeable. Present techniques allow only for the case where the pressure increases and asymptotically approaches the downstream inviscid value.

It is the reattachment process which governs the size, shape, and scale of the separated flow region. Unfortunately, the physical conditions near reattachment are virtually unknown at present.

II-3-4. Coupling Regions Together. The method proposed for coupling the three regions together was mentioned in Section I-3. It has been found experimentally that the shape of the model causing a disturbance is not a variable in determining the pressure rise in the vicinity of the separation point. That is to say, the plateau pressure was found to be independent of the ramp angle for a given Mach number when the Reynolds number at the beginning of the interaction was the same. It is the mixing in the plateau region which is the dominant characteristic in producing the necessary downstream pressure distribution on the ramp. As the ramp angle increases, the plateau region lengthens to accommodate a longer mixing region to produce the higher pressure ratio.

In the Crocco-Lees method, K becomes the "measuring stick" for determining the amount of mixing (just as "a" does in the Lees and Reeves method) for a particular configuration and flow condition. As may be seen in Figure 6, K increases in value as the flow goes from separation to the plateau and then continues on to the shock impingement point. For given initial conditions at the beginning of the interaction, K at the shock is directly related to the size of the ramp angle. A larger ramp angle results in K being larger at the shock, which implies that a longer plateau or mixing region is required.

In the reattachment solution, the magnitude of the pressure rise is related directly to the size of the K change between the shock value and the downstream Blasius value. This points out that a longer plateau region results in a correspondingly greater reattachment pressure rise.

To tie the parts together, K_{sh} must be the value needed to produce the correct reattachment pressure rise. However, K_{sh} is determined by the length of the plateau region which is related to the location of the separation point. Matching conditions at the ramp corner requires adjusting the location of separation. Because of the interplay of the variables which are involved, an iteration solution using the straight dividing streamline is being pursued.

III. EVALUATION OF AVAILABLE EXPERIMENTAL DATA

A current problem common to the study of high velocity laminar separated flows is the availability of only a limited amount of experimental data. An effort was made to obtain and use data from a wide variety of conditions in this study. A total of fourteen cases between Mach 2 and 10 were selected for analysis.

Several problems arise when a correlation is attempted with data from several different facilities and when collected under different conditions. For example, three-dimensional effects become appreciable at higher Mach numbers and depend to a degree upon the tunnel facility.

Analysis of Mach 16 data by Miller et al. (15) was attempted, but the leading edge interaction effects and ε_b values were such that a satisfactory correlation was not possible.

III-1. Tabulation of Data Studied

Table I presents in concise form a digest of the data used and the results obtained from this study. In all cases, a sharp leading edge plate was used. This avoids the interplay of leading edge effects in the interaction region. The pressure distributions from five runs (2,4,6,9, and 13) were selected as representative and are shown in the next section. The results from all fourteen runs were used in order to compare C_1 versus M_∞ (see Section III-3).

The Mach 2.45 case is discussed in considerable detail in Section III-2--since this was the data from which Glick based his results. Several curves showing the pressure distributions and other important characteristics are presented in the next section.

III-2. Element Analysis and Experimental Comparisons

This section is devoted to detailing the techniques used and presenting the results obtained for the different regions. Simplified computer flow diagrams for the three regions are given in Appendix B.

TABLE I. - DATA USED IN ANALYTICAL CORRELATIONS

Item	Run Number						
	1	2	3	4	5	6	7
Mach number	2.0	2.45	2.55	3.0	3.0	4.5	4.5
Reference source	2,4	2,4	16	17	17	18	18
Re/In. x 10^{-4}	15.1	6.0	7.09	3.4	3.6	12.0	8.8
x_b, in.	1.29	.18	.66	4.25	2.6	5.0	4.7
x_s, in.	1.515	.315	1.05	5.7	3.34	5.66	5.5
x_p, in.	1.625	.46	1.30	6.66	4.15	7.30	6.25
x_{sh}, in.	1.96	.90	2.50	8.0	8.0	8.0	8.0
Ramp angle, degrees	a	a	b	10.0	30.0	15.0	15.0
Re_{x_b} x 10^{-4}	19.5	1.08	4.675	14.4	9.36	60.0	41.3
ϵ_b	-.00834	-.0506	-.0272	-.0212	-.0277	-.0371	-.0457
$\lvert\epsilon_b/M_\infty\rvert$	.00417	.0206	.0107	.0071	.00923	.00825	.0102
K_p (approx.)	.685	.755	.735	.730	.755	.750	.750
K_{sh} (approx.)	.785	.890	.885	.805	.910	.785	.810
Approximate C_1 value (Range indicated)	13-14	11-14	10-11	11-13	16-17	13	11-13

[a] Incident shock
[b] Unknown, or no value
[c] No experimental data
[d] Unpublished NASA Langley data

TABLE I. - DATA USED IN ANALYTICAL CORRELATIONS, continued

Item	Run Number						
	8[c]	9	10	11	12	13	14
Mach number	5.8	6.0	8.0	8.0	8.0	8.45	10.03
Reference source	2	d	d	d	d	d	19
Re/In. x 10^{-4}	1.16	10.33	1.835	2.42	3.5	59.0	12.6
x_b, in.	.20	3.0	5.0	5.25	5.0	2.5	3.2
x_s, in.	.54	4.0	7.12	7.5	7.25	3.25	4.0
x_p, in.	.716	6.5	b	b	b	4.5	7.0
x_{sh}, in.	1.25	6.0	10.0	10.0	10.0	6.0	8.7
Ramp angle, degrees	c	14.0	20.0	20.0	20.0	14°36'	30.0
Re_{x_b} x 10^{-4}	2.32	31.0	9.17	12.7	17.5	147.4	40.3
ε_b	-.484	-.129	-.622	-.542	-.454	-.221	-.811
$\lvert \varepsilon_b/M_\infty \rvert$	.0833	.0216	.0778	.0678	.0567	.0262	.0809
K_p (approx.)	.77	.735	.725	.715	.725	.740	.795
K_{sh} (approx.)	.90	.76	.725	.715	.725	.815	.845
Approximate C_1 value (Range indicated)	5.5-6.5	5-7	6-7	7.5-8.5	7-9	5-6	5-6

[a] Incident shock
[b] Unknown, or no value
[c] No experimental data
[d] Unpublished NASA Langley data

III-2-1. Blasius to Separation. The linearized equations which apply between the Blasius point and separation, (10) and (11), were programmed on an IBM 7040. The program requires that values of ε and ζ, analogous to Mach and Reynolds numbers, be chosen for the separation point. Once chosen, these values are used to start the step-by-step claculation which moves upstream to the Blasius point in ΔK increments. The values at the Blasius point are obtained from equations (17) and (18). Repeated choices of ε and ζ at separation must be tried in order to end with the correct values at the Blasius point. The program, through repeated iterations, converges on the desired values of ε and ζ at separation. Once a satisfactory convergence has been obtained, transformation to the real plane is made by using equation (14). The pressure ratios are calculated by using the isentropic relationships.

Figures 7 through 11 illustrate the pressure distributions obtained by this method for five different Mach numbers. In all cases, the separation point was taken to be the value indicated by a Schlieren photograph, or, when that was not given, it was taken to be at the location of the steepest slope in the pressure distribution.

III-2-2. Separation to Ramp Corner. In this region, equations (12) and (13) were programmed for computer solution. The ε and ζ values which had previously been found at separation were used to start the solution. By fixing C_1 as a constant in the separation to plateau region, the program simply marches in ΔK steps, calculating the corresponding pressure ratio and x-location value for each step.

The beginning of the plateau is determined by the pressure gradient becoming zero. Between the beginning of the plateau and the shock, a C(K) was found which makes the pressure gradient remain zero. The solution is terminated when the ramp corner is reached.

Also shown in Figures 7-11 are the pressure distributions in the separation to shock impingement region. The C_1 values which most nearly approximate the experimental distributions are indicated.

In the pressure plateau region, C(K) was allowed to vary in such a manner that a constant pressure ratio resulted. For comparison, Figure 12 illustrates the behavior of C(K) versus K in the plateau region for each of these five cases. It is noted that C(K) increases with K in all cases--serving as an indication that the mixing becomes more vigorous as one moves down the pressure plateau, rather than remaining constant as Glick assumed.

III-2-3. Reattachment. A computer program incorporating the discussion in Section II-1-1 (Reattachment) was used for this region. In general, to obtain the correct magnitude for the reattachment pressure rise, a K_{sh} value larger than that generated in the Separation-Shock Impingement computation was needed.

Figure 13 illustrates the reattachment solution obtained for the Mach 3.0 case which previously was shown in Figure 8. In order to get the plateau and reattachment regions to join, a longer plateau mixing region would be needed (to produce a larger K_{sh} value). Because there are some apparent difficulties in the reattachment solution, correlations were attempted only at Mach 2.45 and 3.0.

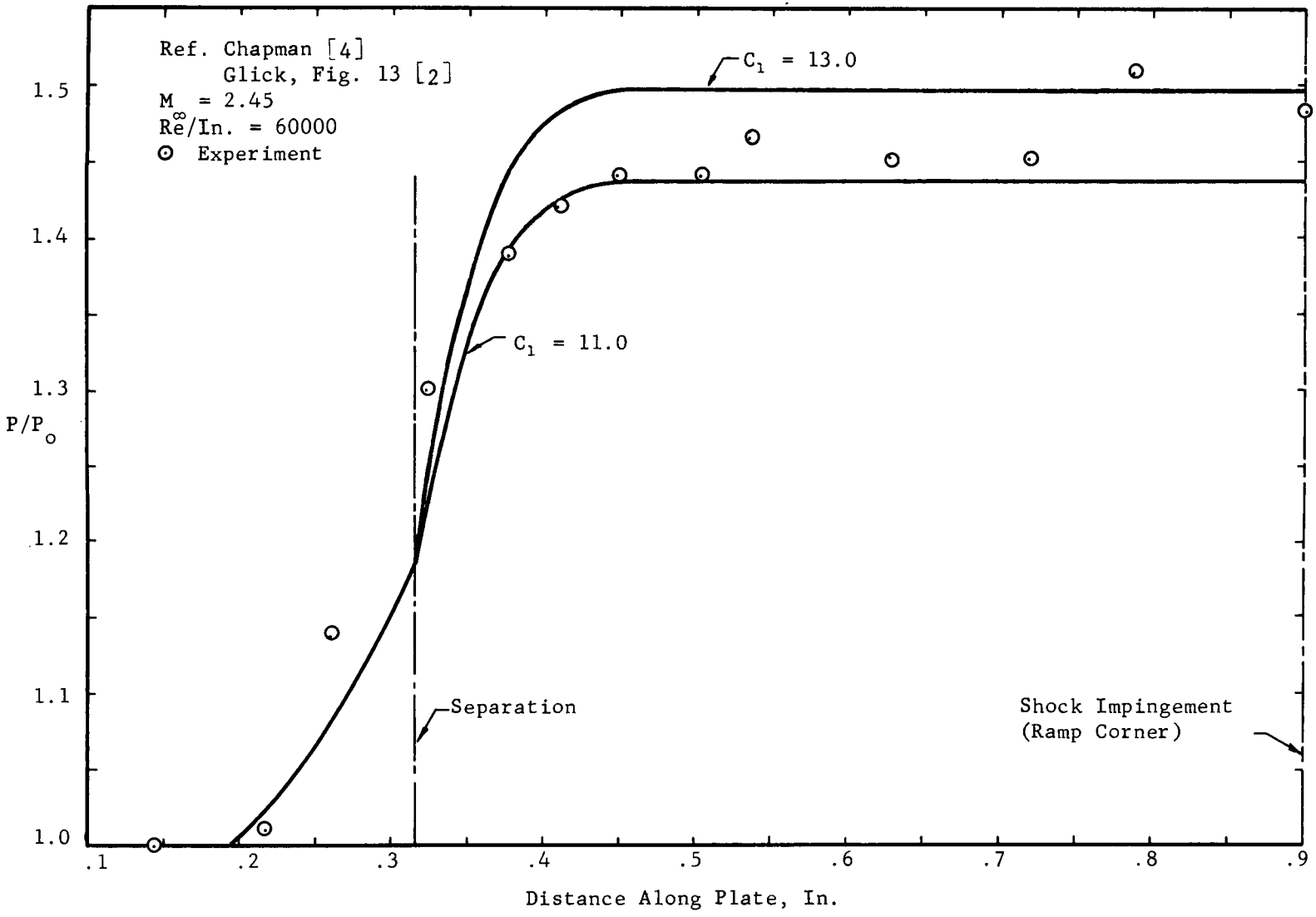

Figure 7. Pressure Correlation At Mach 2.45
(Blasius-Shock Impingement)

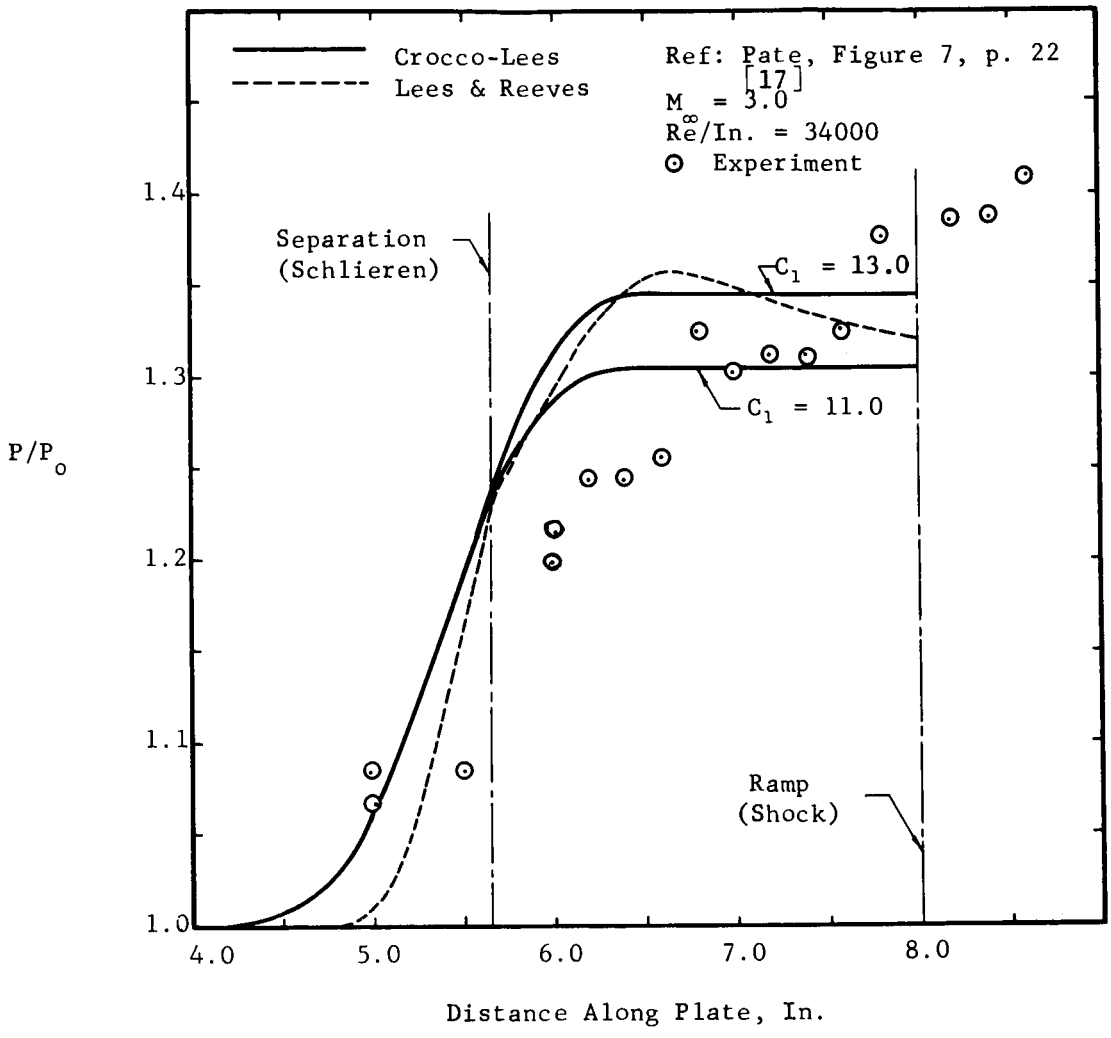

Figure 8. Pressure Correlation at Mach 3.0 (Blasius-Shock Impingement)

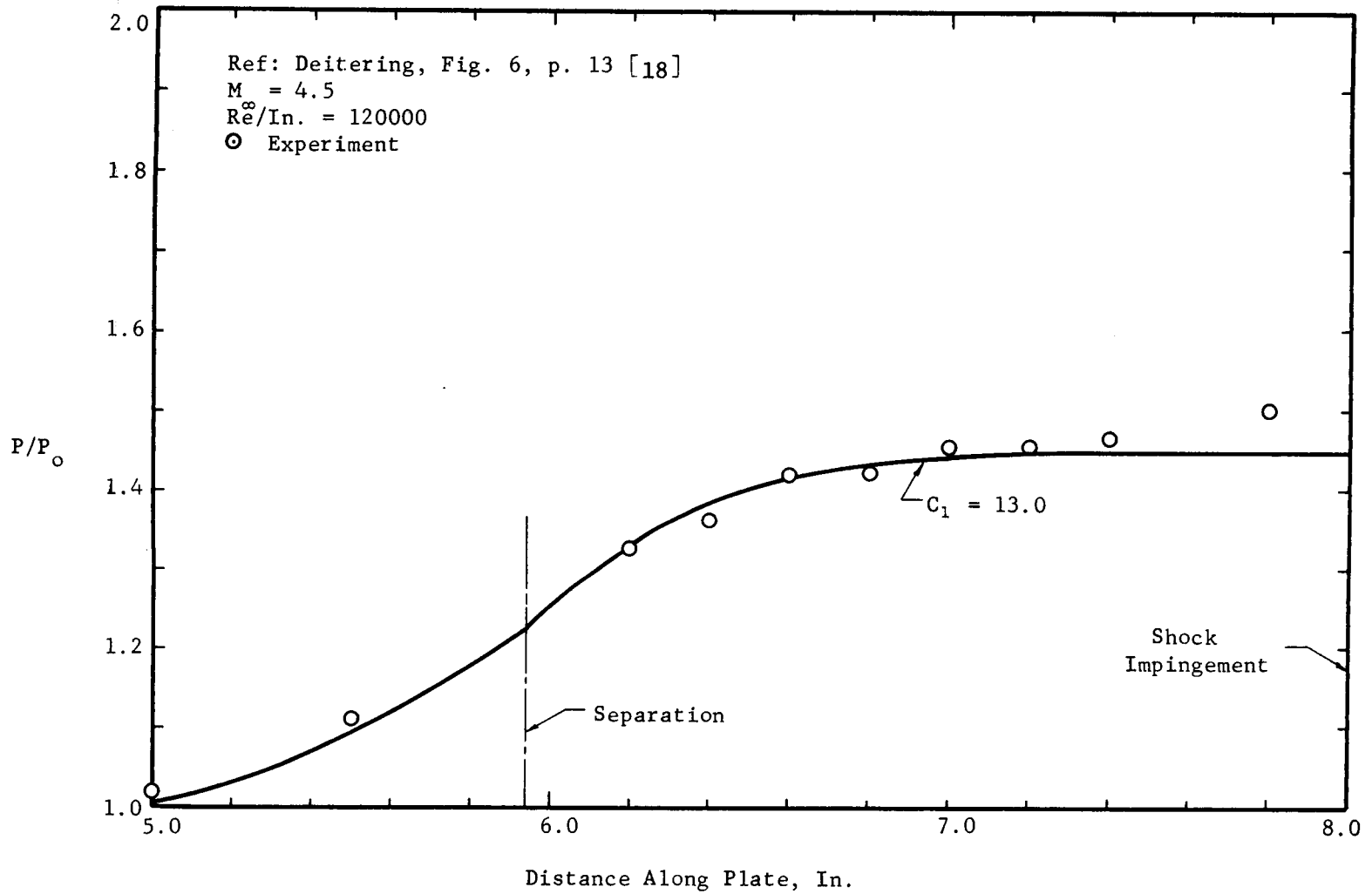

Figure 9. Pressure Correlation at Mach 4.5

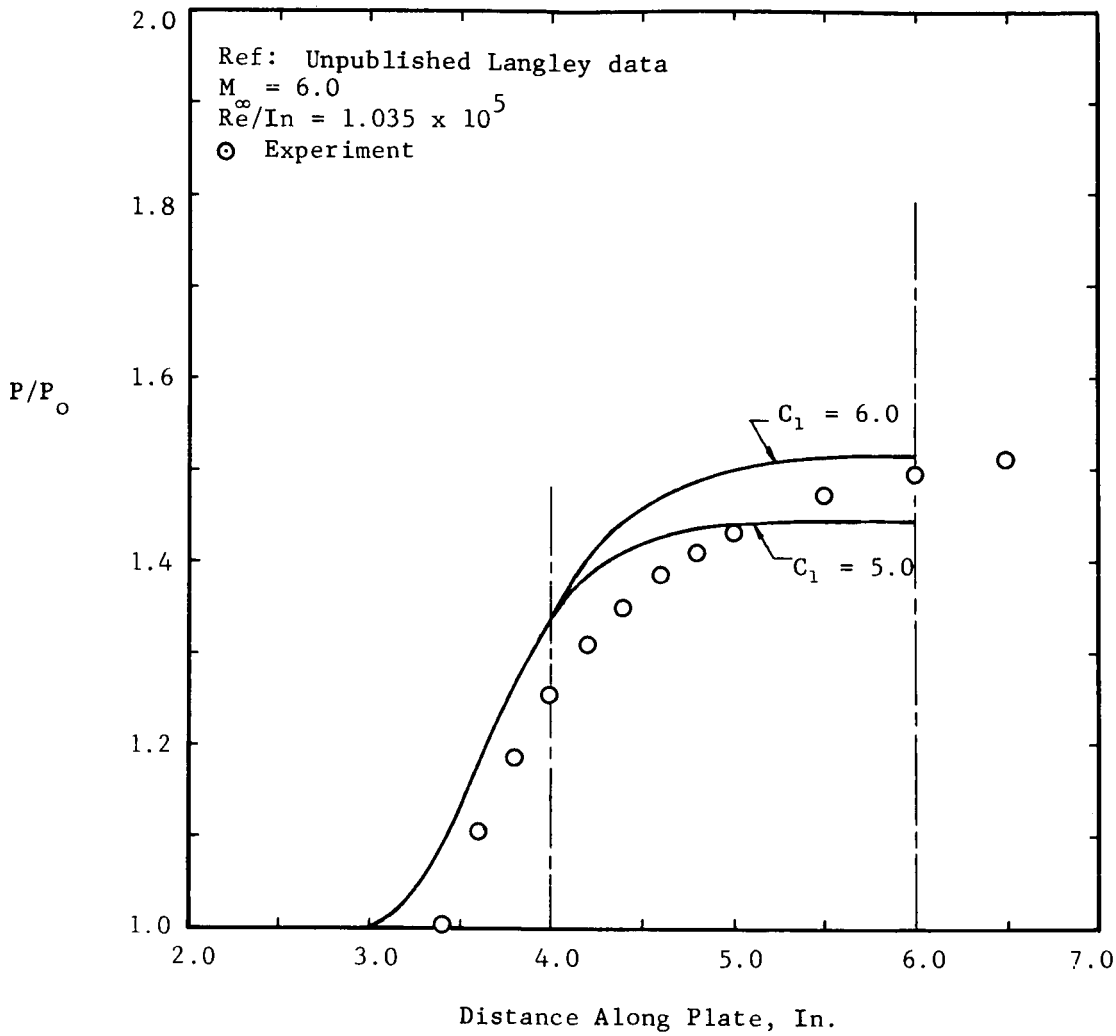

Figure 10. Pressure Correlation at Mach 6.0

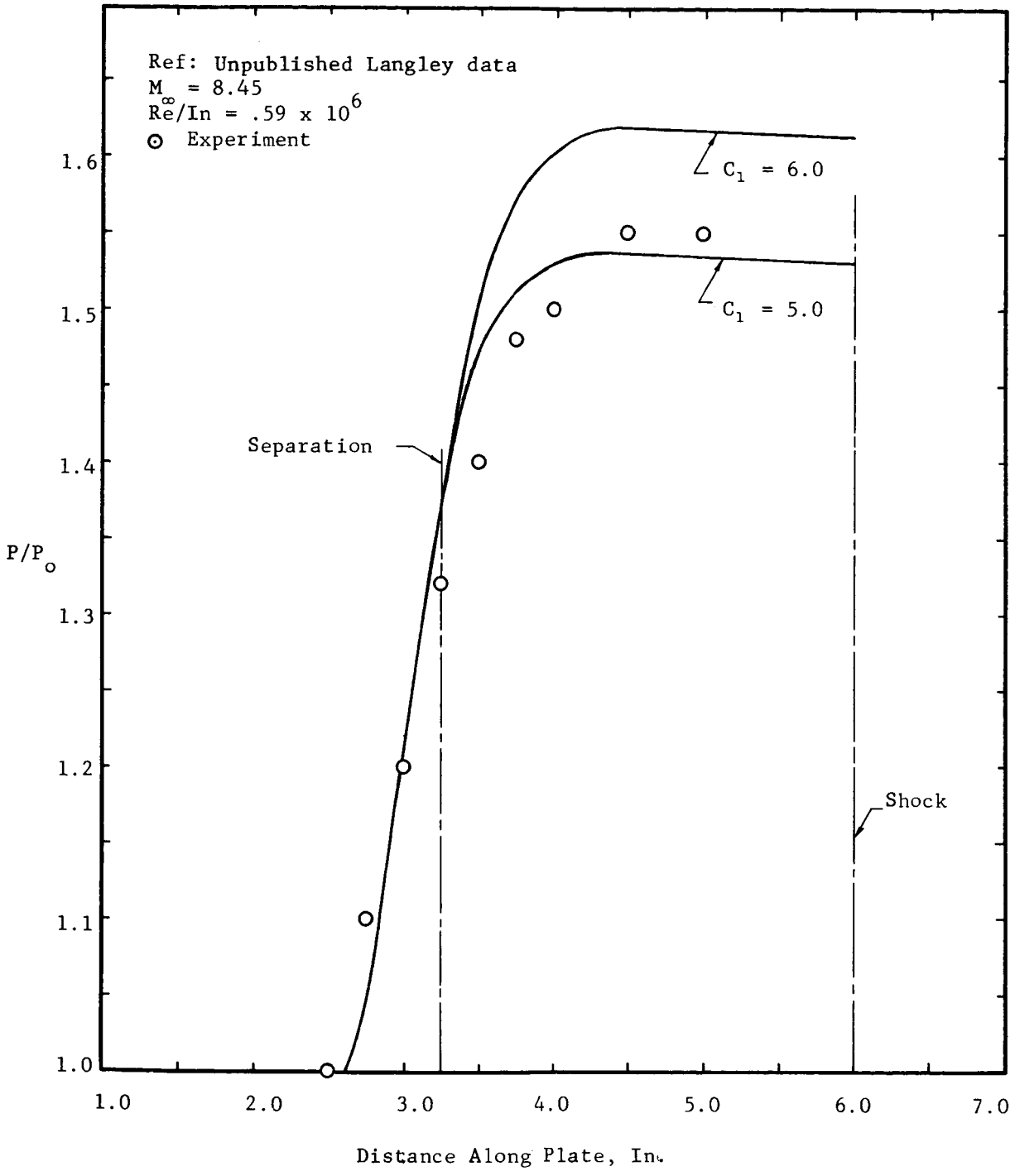

Figure 11. Pressure Correlation at Mach 8.45

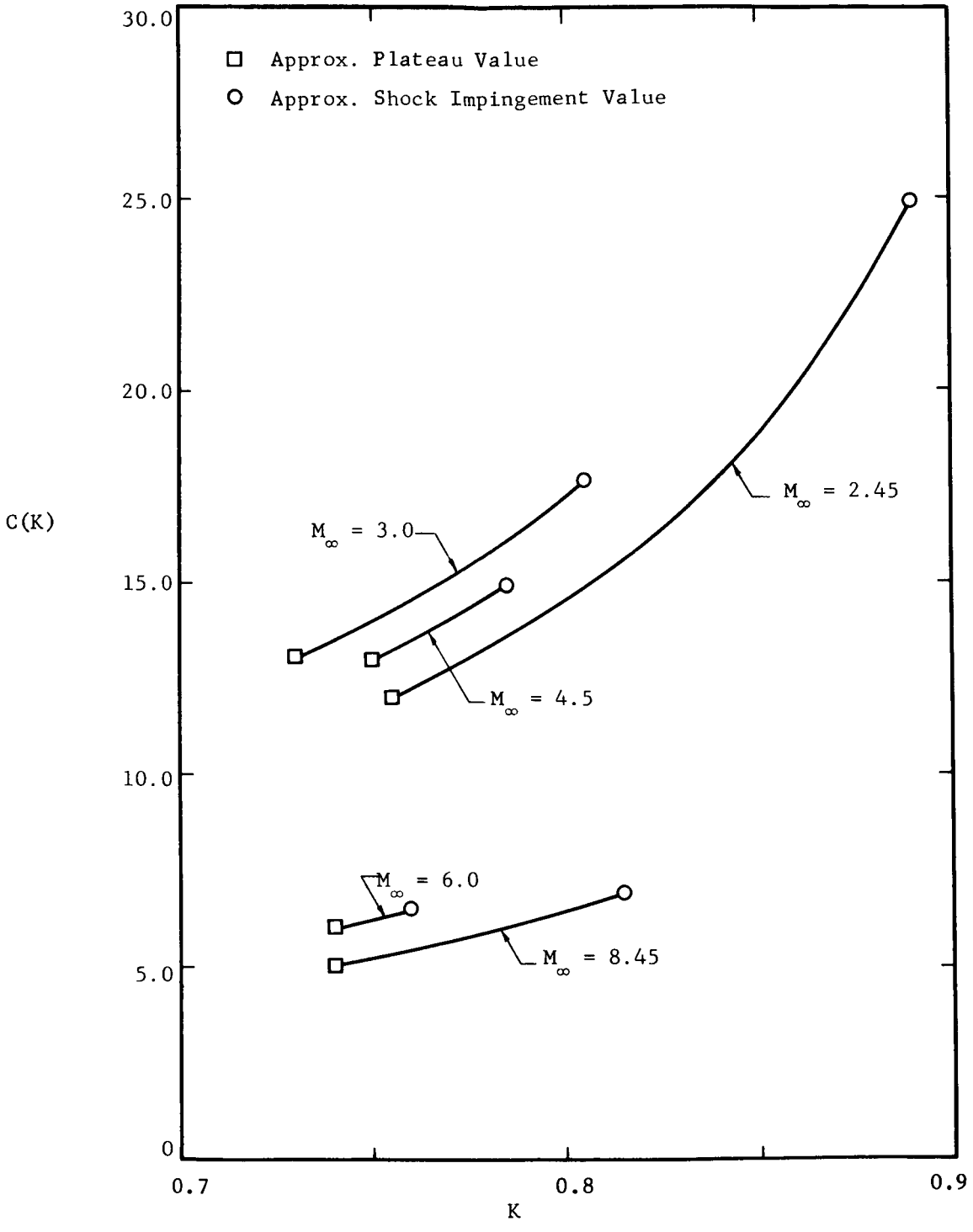

Figure 12. C(K) vs. K in Plateau Region for Different Mach Numbers

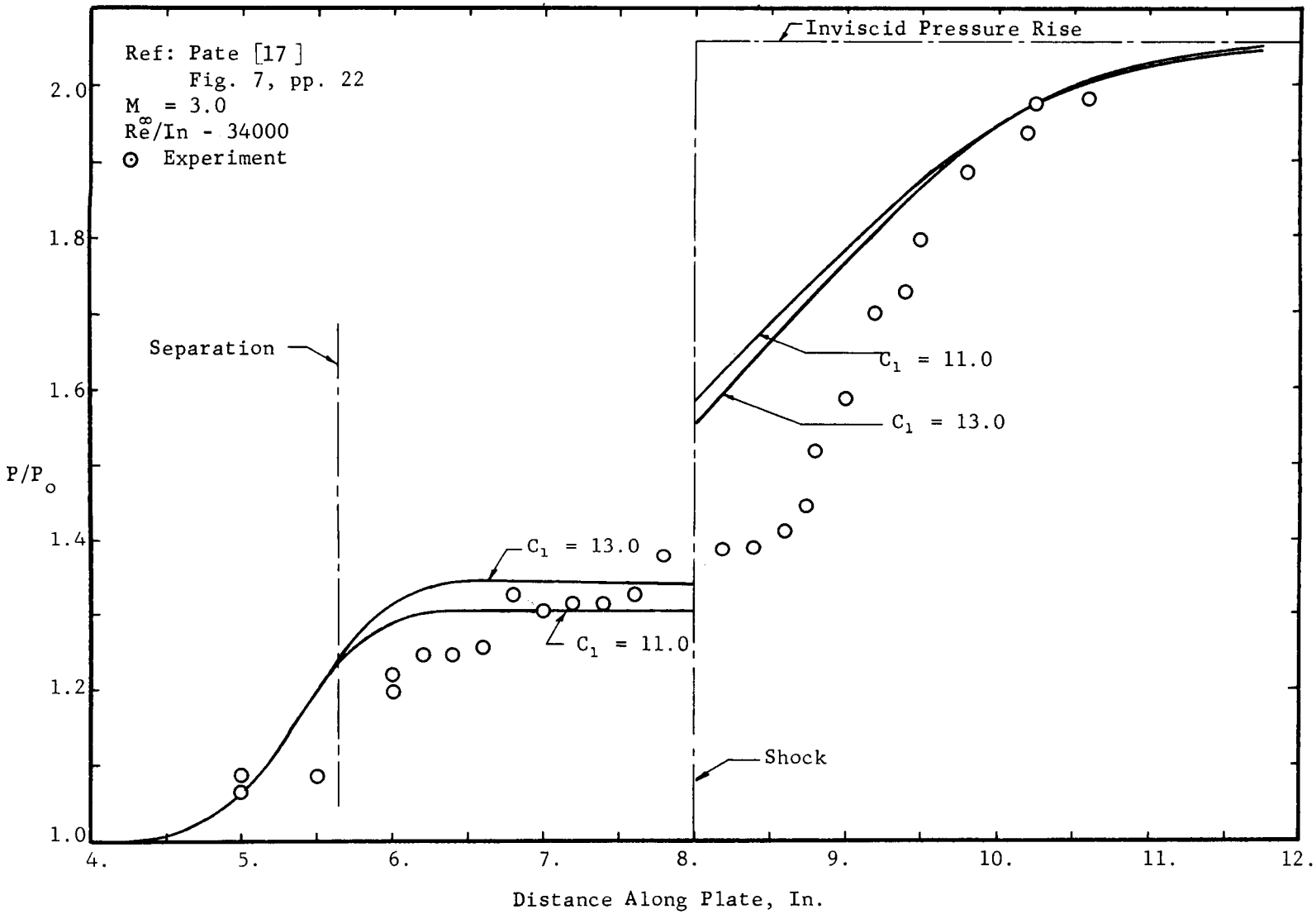

Figure 13. Pressure Correlation for Entire Interaction at Mach 3.0

III-2-4. Coupling of Regions. An effort was made to couple the regions together, and in particular to duplicate the Mach 2.45 solution which Glick reports. Figure 14 depicts the entire interaction region for Mach 2.45 and shows both Glick's curve and the curve obtained from this study--using the same inputs as Glick. By using $C_1 = 11.0$ and $C_2 = 15.0$, the present study produced a somewhat different distribution. The K_{sh} obtained in this study correlated closely with Glick's value for K_{sh}, but the resulting reattachment pressure distribution is different. A considerable discontinuity at the ramp corner is noted in the present study.

In an attempt to reproduce Glick's Mach 5.8 curve, $C_1 = 11.0$ was found to not be a "universal" value. In this case, a C_1 value of approximately 5.0 was needed to attain the proper pressure plateau ratio, which disagrees with Glick's conclusions.

Figure 15 gives a visual display of how the three semi-empirical factors F(K), D(K) and C(K) behave throughout the treatment which has just been outlined. The C(K) trajectory shown isn't the optimum one, but it quantitatively accounts for the pressure distribution ahead of the ramp corner. Refinements in C(K), particularly in the reattachment region, now seem to be needed to correct the mismatch in pressure ratios which now exist at the ramp corner.

As a comparison, the Lees and Reeves (5) calculations were performed for the Mach 3.0 case and the results appear in Figure 8. The technique for solution is similar to that outlined in Sections III-2-1 and III-2-2 for Glick. The convergence at the Blasius point was found to be very sensitive to the $\delta^*_{t_s}$ value chosen. The difficulty apparent in Figure 8 is the occurrence of a peak pressure in the plateau region. This may be a result of unsatisfactory accuracy in the Blasius point convergence.

III-3. Effect of Mach and Reynolds Numbers on C(K)

One objective of this study was to correlate the dependence of C_1 upon the Mach and Reynolds number at the beginning of the interaction. This goal has not been accomplished to the satisfaction of the investigators--due primarily to the limited variation of Reynolds number in the data treated. It is hoped that this will be overcome in the near future.

Since only sharp leading edges were considered, the free stream Mach number and the local Mach number at the beginning of the interaction are nearly the same--provided that the Reynolds numbers aren't too low. Figure 16 shows a correlation of M_∞ versus C_1, based upon the values presented in Table I. A curve has been drawn which represents a crude correlation of C_1 versus M_∞. From necessity, the dependence of C_1 upon Reynolds number is taken as second order and neglected in the correlation. It is felt that there is a Reynolds number dependence, but that it cannot be established until more data has been analyzed.

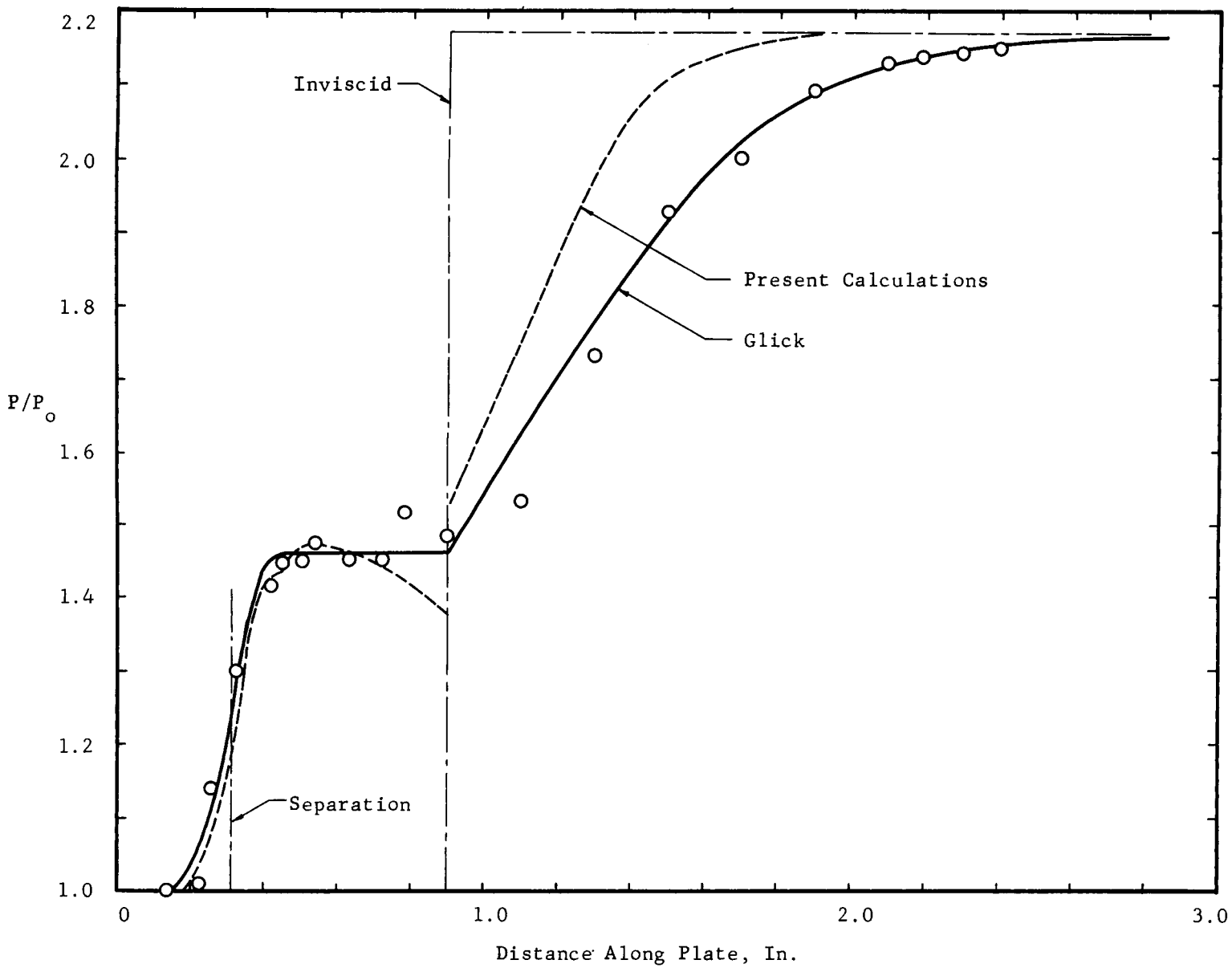

Figure 14. Comparison of Calculations With Glick's Results for $C_1 = 11.0$, $C_2 = 15.0$

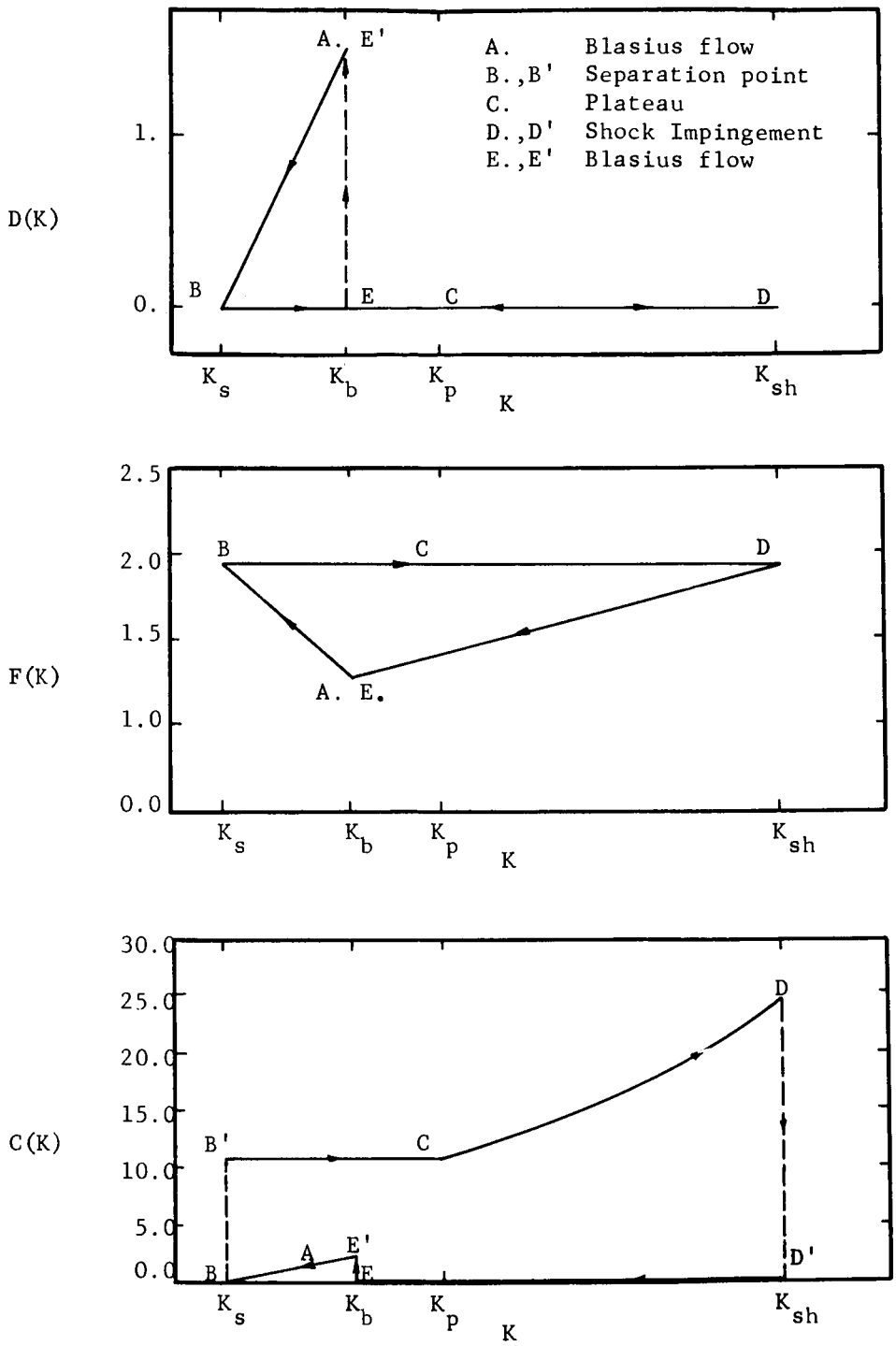

Figure 15. Trajectories of Semi-Empirical Parameters in a Shock Wave-Laminar Boundary Layer Interaction

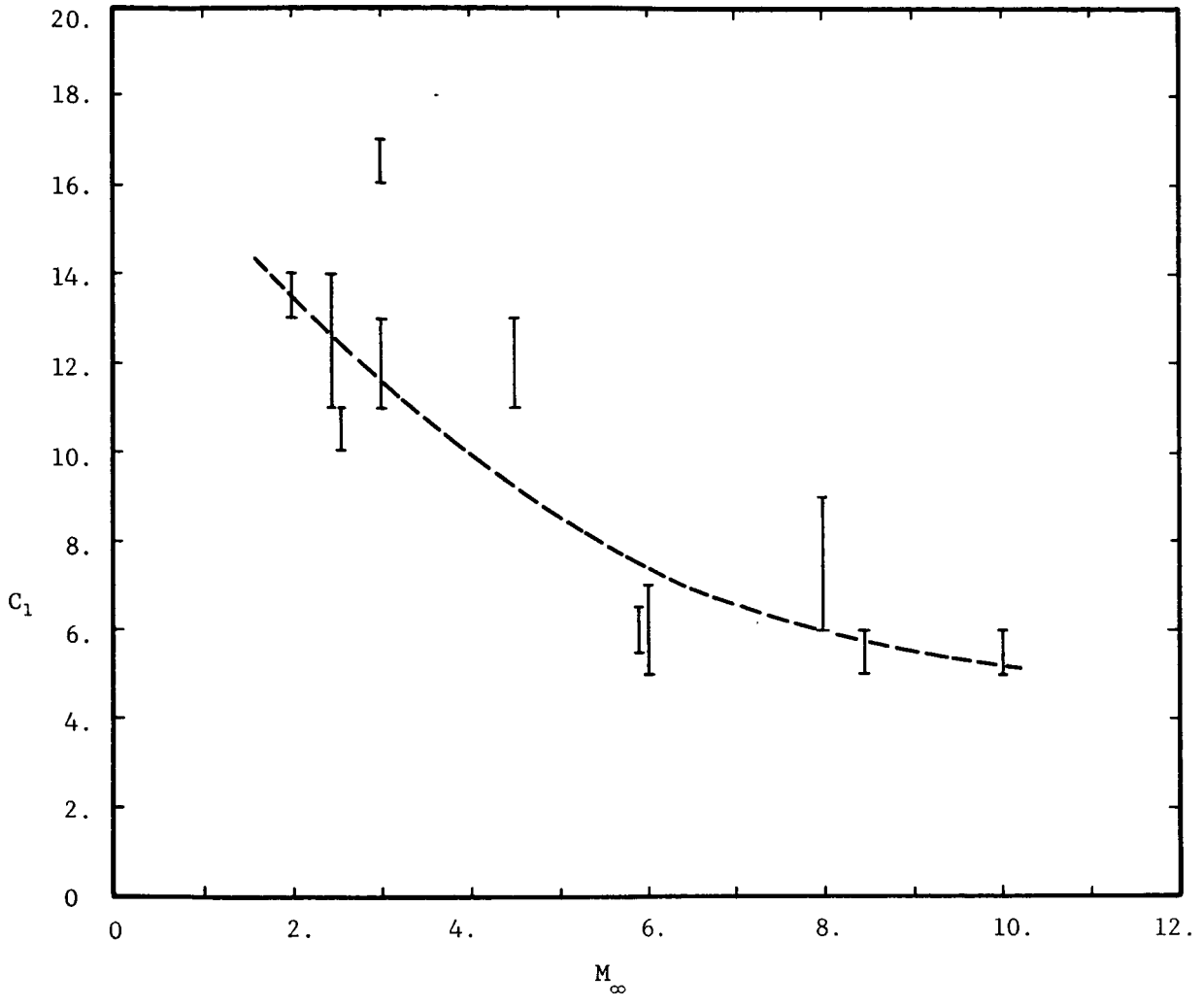

Figure 16. C_l vs. M_∞ for Shock Induced Laminar Boundary Layer Separations

III-4. Miscellaneous

Future work will include refinements in the numerical integration technique. Euler's method has been used on all the work to date except for the Lees and Reeves solution in which a fourth order Runge-Kutta method was used. Now that the general trends and problems in the solution have been established, a fourth order Runge-Kutta method of integration is planned. This should improve the accuracy without altering the conclusions already reached.

A study by Chapman (4) concluded that in the reattachment region the mixing was zero for the model used. The mixing in this region is expected to be small, but not zero. On this basis, the reattachment solution must begin from a new form of the momentum equation, considerably different from the one presently being used. Figure 17 illustrates a possible trajectory for C(K), depicting a different behavior in the reattachment region.

The difficulties in treating rounded leading edges has not been overcome. Hayes and Probstein (20) define an interaction parameter and correlate this with both weak and strong interactions (sharp and blunted leading edges respectively). This leading edge effect coupled with the interaction is being investigated.

IV. SUMMARY AND CONCLUSIONS

IV-1. Principal Results

The present study, while clarifying the understanding up to the shock location, does not solve the overall interaction. Much of the needed correlation must await the availability of more experimental data. The following important points are reiterated to summarize the work that was done:

1. The interaction region prior to shock impingement (or ramp corner) has been studied in detail to determine the behavior of the semi-empirical correlation factors for the Crocco-Lees and Glick methods. It was found that C(K) was not a "universal" quantity, as Glick has proposed. In particular, a dependence of C_1 upon Mach number in the range from 2 to 10 was proposed. The F(K) and D(K) relations which were used are to be regarded only as first approximations.

2. As noted just above, as a first approximation, C_1 has been found as a function of Mach number only. As more experimental data is analyzed, a dependence of C(K) on both Me_b and Re_b is anticipated.

3. C(K) was found to be an increasing function in the plateau region, rather than remaining constant as was previously concluded.

4. The technique for incorporating the whole interaction within a single framework has been discussed. Further work on the reattachment solution is needed before this can be completed.

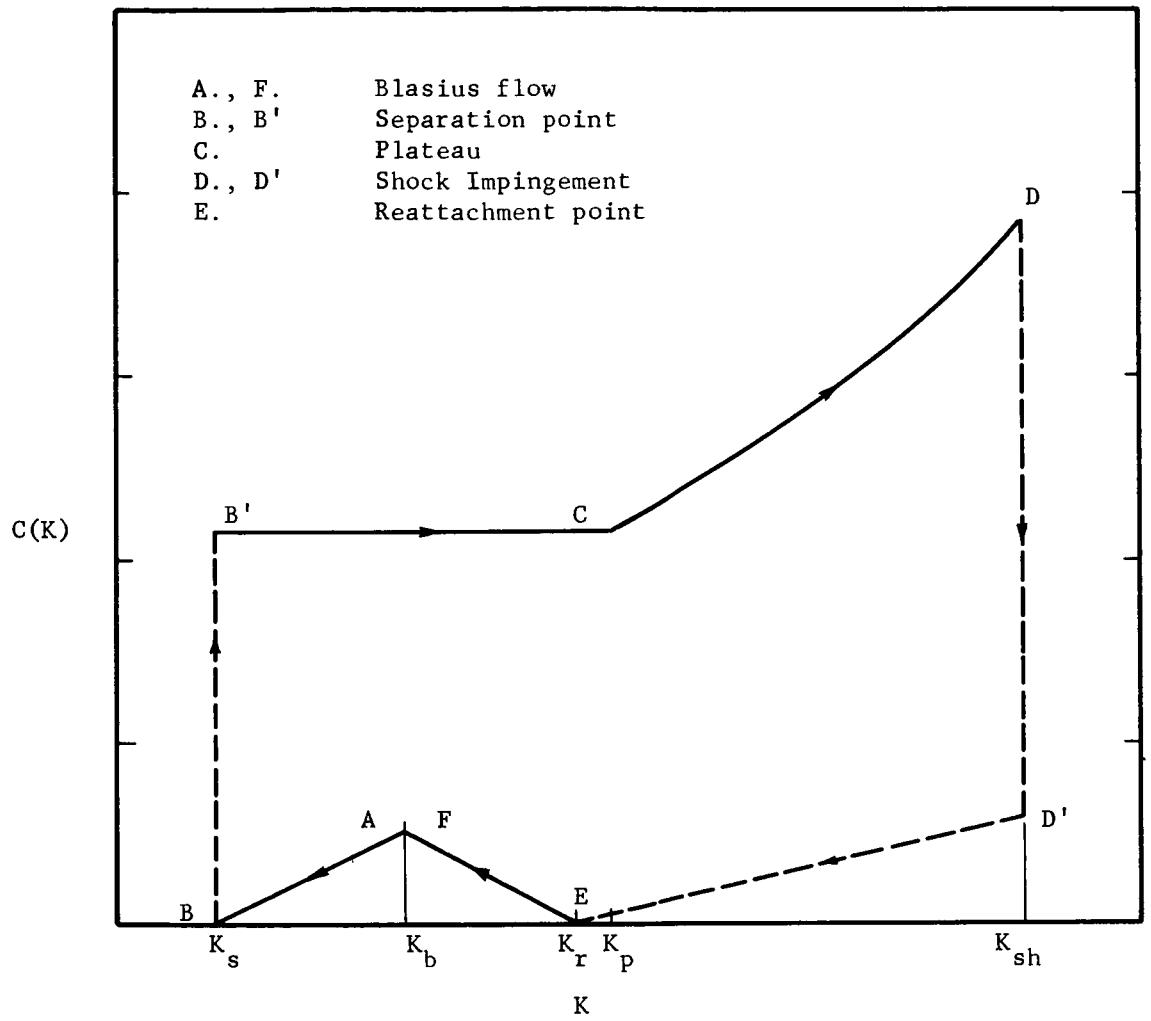

Figure 17. Proposed C(K) Trajectory

5. The linearization limitations were discussed. Figure 5 shows the effects that Mach and Reynolds number have on these assumptions. A high Mach number, or low Reynolds number, or a combination of these conditions can produce results which invalidate the linearization assumption that $\varepsilon << M_\infty$.

IV-2. Recommendations for Future Study

In addition to coupling the entire flow interaction together and refining the numerical integration technique, the following recommendations are offered:

1. Remove the linearization which has been placed on the equations which apply ahead of the ramp corner or shock impingement point. This would necessitate using the local Mach number rather than the free stream value in the calculations. In a computer solution, this should pose no great difficulty.

2. An effort should be made to measure experimentally velocity profiles in the separated region. This would be helpful in establishing K characteristics for the flow throughout the separated portion of the interaction. Additionally, f and K calculations at supersonic speeds, based upon measured attached and separated profiles, would lend considerable support to a refined understanding of F(K).

REFERENCES

1. Crocco, L., and Lees, L.: A Mixing Theory for the Interaction Between Dissipative Flows and Nearly Isentropic Streams, Journal of the Aeronautical Sciences, Vol. 19, No. 10, pp. 649-676, October, 1952.

2. Glick, Herbert S.: Modified Crocco-Lees Mixing Theory for Supersonic Separated and Reattaching Flows, CAL TECH Hypersonic Research Project Memo. No. 53, (May 2,1960); also, Journal of the Aeronautical Sciences, Vol. 29, pp. 1238-1249, Oct. 1962.

3. Stewartson, K.: Correlated Incompressible and Compressible Boundary Layers, Proc. Roy. Soc., London, Vol. 200, pp. 84-100, 1949.

4. Chapman, D. R., Kuehn, D. M., and Larson, H. K.: Investigation of Separated Flows in Supersonic and Subsonic Streams with Emphasis on the Effects of Transition, NACA Report 1356, 1958.

5. Lees, L. and Reeves, B. L.: Supersonic Separated and Reattaching Laminar Flows, I. General Theory and Application to Adiabatic Boundary-Layer/ Shock Wave Interactions, AIAA Journal, Vol. 2, No. 11, pp. 1907-1920, Nov. 1964; also, GALCIT Separated Flows Research Project, Tech. Report No. 3, Oct. 1963.

6. Stewartson, K: Further Solutions of the Falkner-Skan Equation, Proc. Cambridge Phil. Soc., Vol. 50, pp. 454-465, 1954.

7. Cohen, C. B., and Reshotko, E.: Similar Solutions for the Compressible Laminar Boundary Layer with Heat Transfer and Pressure Gradient, NACA Report 1293, 1956.

8. Dorodnitsyn, A. A.: General Method of Integral Relations and Its Application to Boundary Layer Theory, Advances in Aeronautical Sciences, Pergamon Press, Vol. 3, pp. 207-219, 1962.

9. Nielsen, J. N., Lynes, L. L., Goodwin, F. K., and Holt, M.: Calculation of Laminar Separations with Free Interaction by the Method of Integral Relations, Submitted for presentation at the AIAA 2nd Aerospace Sciences Meeting, January 25-27, 1965, in New York City, Vidya Research and Development, 1450 Page Mill Road, Palo Alto, Calif.

10. Erdos, J. and Pallone, A.: Shock-Boundary Layer Interaction and Flow Separation, AVCO Technical Report RAD-TR-61-23, August 15, 1961.

11. Pinkus, O.: A Method of Solving Supersonic Laminar Boundary-Layer Separation and Its Application to Wedges and Curved Surfaces, RAC 2232A, Republic Aviation Corp., Framingdale, L. I., N. Y.,; also, ASME Paper No. 65-APMW-19, 1965.

12. Tani, I.: On the Approximate Solution of the Laminar Boundary Layer Equations, Journal of the Aeronautical Sciences, Vol. 21, pp. 487-504, July 1954.

13. Makofski, R. A.: A Two-Parameter Method for Shock Wave-Laminar Boundary Layer Interaction and Flow Separation, Proceedings of the 1963 Heat Transfer and Fluid Mechanics Institute, Pasadena, Calif. June 12-14. 1963.

14. Gulbran, C. E., Redeker, E., Miller, D. S., and Strack, S. L.: Heating in Regions of Interfering Flow Fields, Part I. Two - and Three-Dimensional Laminar Interactions at Mach 8, AFFDL-TR-65-49, Part I, July 23, 1965.

15. Miller, D. S., Hijman, R., and Childs, M. E.: Mach 8 and 22 Studies of Flow Separation Due to Deflected Control Surfaces, AIAA Journal, Vol. 2, pp. 312-321, February, 1964.

16. Nielsen, J. N., Lynes, L. L., and Goodwin, F. K.: Theory of Laminar Separated Flows on Flared Surfaces Including Supersonic Flow with Heating and Cooling, AGARD Conference Proceedings No. 4, Separated Flows, 1966.

17. Pate, S. R.: Investigation of Flow Separation on a Two-Dimensional Flat Plate Having a Variable-Span Trailing-Edge Flap at M_∞ = 3 and 5, Report No. AEDC-TDR-64-14, March 1964.

18. Deitering, J. S.: Investigation of Flow Separation on a Two-Dimensional Flat Plate Having a Variable-Span Trailing-Edge Flap at M_∞ = 3 and 4.5, AEDC-TR-65-59, March, 1965.

19. Townsend, J. C.: Effects of Leading-Edge Bluntness and Ramp Deflection Angle on Laminar Boundary-Layer Separation in Hypersonic Flow, NASA TN D-3290, February, 1966.

20. Hayes, W. D., and Probstein, R. F.: Hypersonic Flow Theory, Academic Press, New York and London, Chapter IX, 1959.

ADDITIONAL REFERENCES

1. Le Blanc, L. P., and Webb, H. G. Jr.: Boundary Layer Separation in a Supersonic Stream, Report SID 61-72, Space and Information Systems Division, North American Aviation, Inc., March 29, 1961.

2. Wuerer, J. E., and Clayton, F. I.: Flow Separation in High Speed Flight, A review of the State-of-the-Art, Douglas Report SM-46429, April, 1965.

3. Kaufman, L. G., Meckler, L., Hartofilis, S. A., and Weiss, D.: An Investigation of Hypersonic Flow Separation and Control Characteristics, AFFDL-TR-64-174, January, 1965.

4. Hakkinen, R. J., Greber, I., Trilling, L., and Abarbanel, S. S.: The Interaction of an Oblique Shock Wave with a Laminar Boundary Layer, NASA Memo. 2-18-59W, 1959.

NOMENCLATURE

a	velocity profile parameter, speed of sound
b	velocity profile parameter (Makofski)
$C(K)$	mixing rate correlation function
$\bar{C}$, C_1, C_2	average values of $C(K)$
c_f	skin friction coefficient
$D(K)$	skin friction correlation function
f	defined in equation (3)
F, $F(K)$	defined in equation (7)
I	momentum flux = $\int_0^\delta \rho u^2 dy$
k	$(d\delta/dx) - \theta$
L,N,P,Q	arbitrary parameters in equations (10) and (11)
$\bar{m}$	mass flux in the x-direction = $\int_0^\delta \rho u dy$
m	$\bar{m}\, a_t$
M	Mach number
N_1, N_2, N_3, dH/da	parameters in Lees and Reeves method
p	pressure
Re	Reynolds number
T	temperature
t	$T_e/T_t = (1 - \frac{\gamma-1}{2} w_e^2)$
u	velocity in x-direction
w	u/a_t
x, y	coordinates along, and normal to, the wall
γ	ratio of specific heats
δ	boundary layer thickness
δ^*	displacement thickness

δ_t^*	transformed displacement thickness (Lees and Reeves)
δ^*	momentum thickness
ε	$M_e - M_\infty$
ζ	$m/\mu_t a_t$
K	Crocco-Lees velocity profile parameter
μ	coefficient of viscosity
ρ	density
ϕ_e	$\frac{(1-\frac{\gamma-1}{2} w_e^2)}{\gamma w_e}$
ϕ_1	$(T_1/T/_t)(1/\gamma w_1)$
θ	Streamline direction relative to the wall at $y = \delta$
σ	$\frac{D(K)}{2(1 - K)\ C(K)}$

Subscripts

b	Blasius flat plate conditions
e	conditions at $y = \delta$
i	incompressible conditions
Γ, p, plat	plateau
r	reattachment point
s	conditions at separation
sh	conditions at shock impingement
t	free stream stagnation conditions
x	at location x
1	mean value of viscous region
∞	free stream conditions

APPENDIX A

OTHER ANALYTICAL METHODS

Dorodnitsyn

In the continuing review of literature the Dorodnitsyn method (11, 12) is found to be mentioned with greater frequency. This technique, a general method of numerical solution for nonlinear hydrodynamic problems, is often refered to as the "method of integral relations" and has the important advantage of being well-suited for digital computation. The method is new and promising, but has some inherent difficulties. Principal among these is the fact that the one-parameter family of velocity profiles used does not accurately represent all the possible velocity profiles that can be developed in separated and attached flows.

Erdos and Pallone

The method given by Erdos and Pallone (13) deals specifically with the separation caused by a compression corner in supersonic flow. This method makes use of the concept of a "free interaction" for both laminar and turbulent flows. The analysis treats this complex separation phenomenon in two phases:

1. A study of shock-boundary layer interaction (without specification of the location of the interaction with respect to the compression corner.)

2. Application of the results of the first phase to the problem of flow separation in a compression corner, and determination of the location of the separation and reattachment interaction.

The results of the free interaction theory provide a means of predicting the occurrence of separation and the pressure distribution in the vicinity of the separation point (and possibly the reattachment point), but they do not locate the separated flow with respect to the geometry that originally caused the separation. These semi-empirical equations for the pressure distribution in the "free interaction" are strictly applicable only for perfect gases.

The location of the separation and reattachment points has been fixed by an empirical correlation formula. With the correlation formula and the "free interaction" equations, it is possible to predict the complete pressure distribution for a shock-separated flow. However, a limitatation mentioned is that this correlation formula is based upon very meager data, a single experiment, and is only a first approximation. Additional data is needed to confirm and extend the results.

Pinkus Method

A system of equations was developed by Pinkus (14) which applies to the case of separated laminar boundary layers on compression corners and curved surfaces. This method is an extension of Tani's (15) work, which had applied only to attached flows. Both methods use a quartic velocity profile and make use of the moment-of-momentum boundary layer equation. The profiles are defined in terms of an arbitrary parameter "a" which has physical meaning in that it is proportional to the shearing stress at the wall.

The separated boundary layer is divided into three regions: the detachment, central, and reattachment. The end conditions at the reattachment point impose the constraining restrictions on the solution when the three regions are combined.

Makofski Method

The Makofski (16) method uses a modified Pohlhausen approach with the velocity distribution represented by a fifth-degree polynomial with two undetermined parameters. One of the parameters is related to the skin friction at the wall, while the other is proportional to the imposed pressure gradient.

The method of analysis used consists of transforming the compressible laminar boundary layer equations into incompressible form, obtaining the integral relations, and finally, solving these relations by use of the fifth-degree polynomial. The parameters a and b which describe the velocity profiles are dependent only upon the local Mach number and Reynolds number and are independent of the agency causing the disturbance.

As with other methods using the Pohlhausen approach, the primary difficulty lies in its application to the constant pressure plateau region downstream of separation. There are additional mathematical complexities in the two-parameter approach--the only justification being the possibility of obtaining significantly better results. At higher Mach numbers where three-dimensional effects are significant, it is possible that a two-parameter approach may be needed.

APPENDIX B

SIMPLIFIED COMPUTER FLOW DIAGRAMS

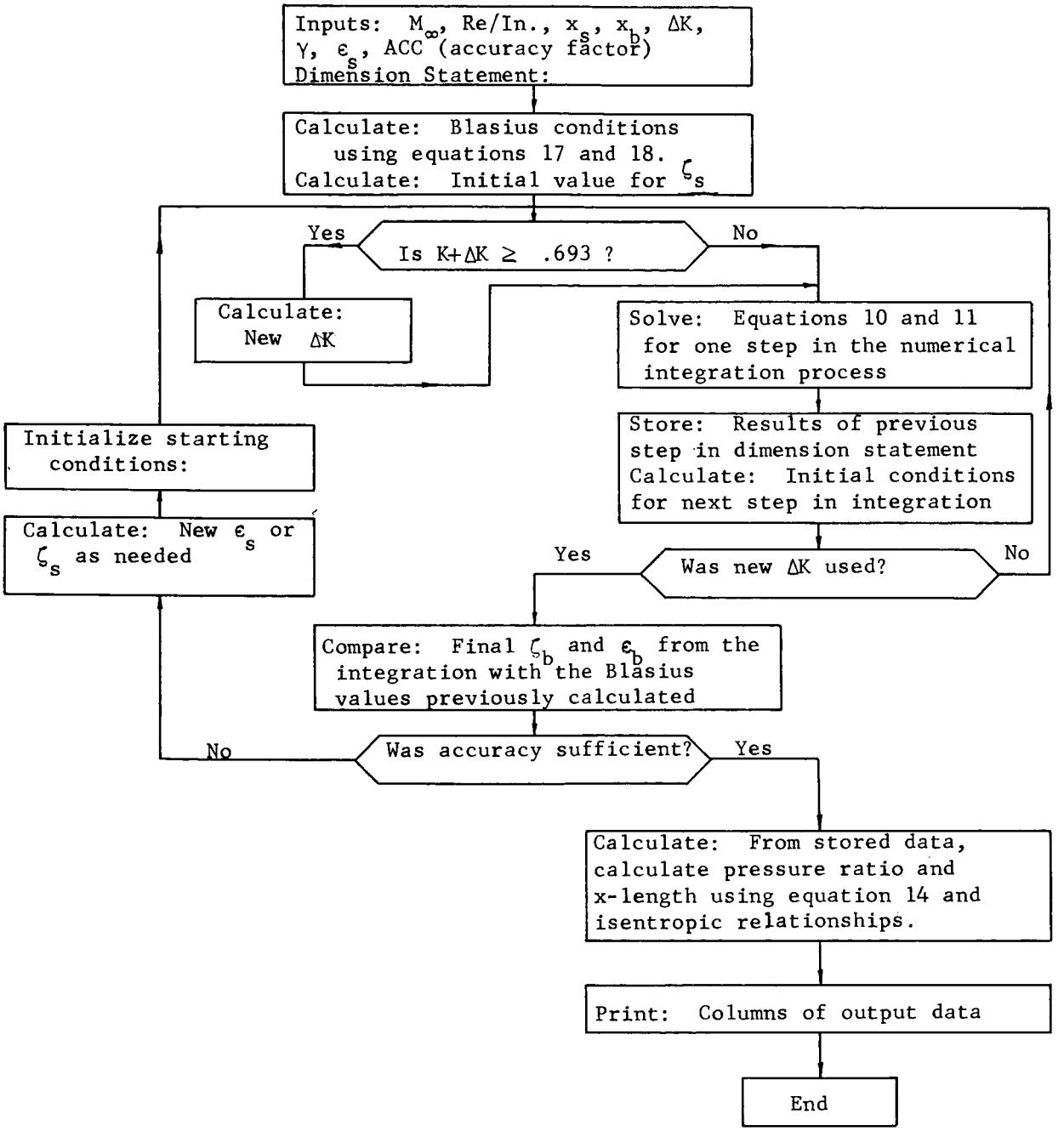

Figure 18. Simplified Flow Diagram for Crocco-Lees Method (Blasius Flow - Separation Point)

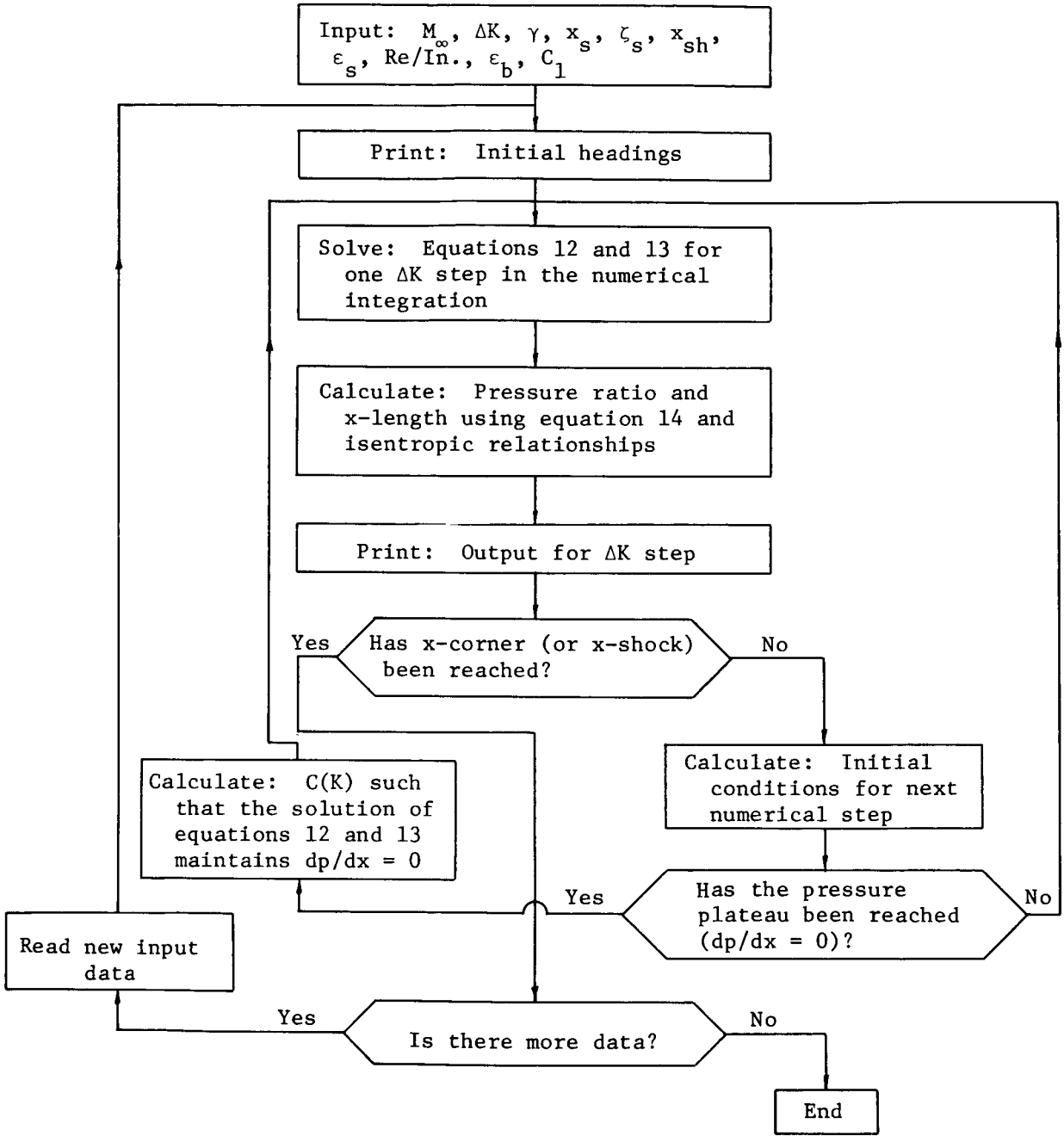

Figure 19. Simplified Flow Diagram for Crocco-Lees Method (Separation Point - Shock Impingement)

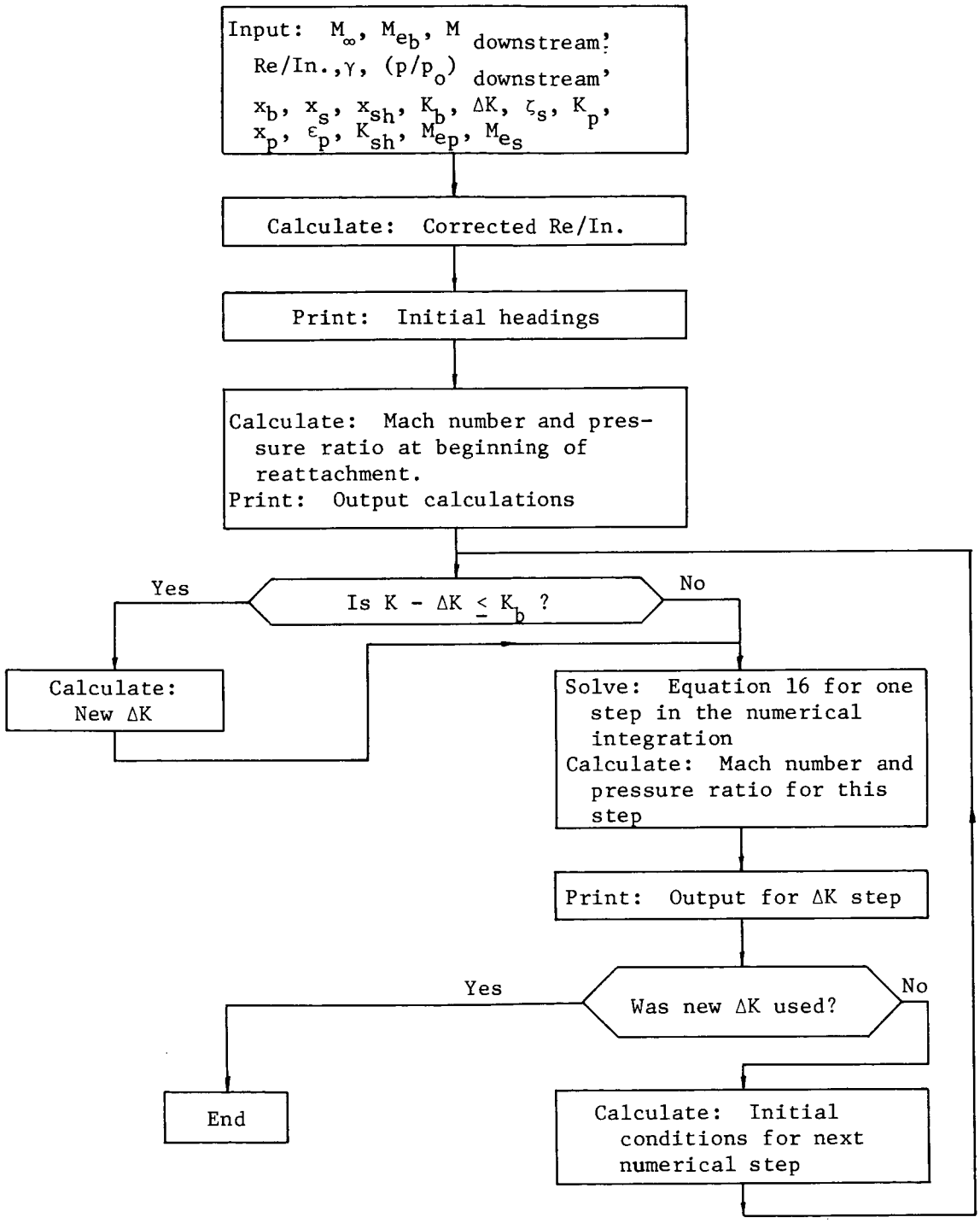

Figure 20. Simplified Flow Diagram for Crocco-Lees Method (Reattachment)

10-5-67

"The aeronautical and space activities of the United States shall be conducted so as to contribute . . . to the expansion of human knowledge of phenomena in the atmosphere and space. The Administration shall provide for the widest practicable and appropriate dissemination of information concerning its activities and the results thereof."

—NATIONAL AERONAUTICS AND SPACE ACT OF 1958

NASA SCIENTIFIC AND TECHNICAL PUBLICATIONS

TECHNICAL REPORTS: Scientific and technical information considered important, complete, and a lasting contribution to existing knowledge.

TECHNICAL NOTES: Information less broad in scope but nevertheless of importance as a contribution to existing knowledge.

TECHNICAL MEMORANDUMS: Information receiving limited distribution because of preliminary data, security classification, or other reasons.

CONTRACTOR REPORTS: Scientific and technical information generated under a NASA contract or grant and considered an important contribution to existing knowledge.

TECHNICAL TRANSLATIONS: Information published in a foreign language considered to merit NASA distribution in English.

SPECIAL PUBLICATIONS: Information derived from or of value to NASA activities. Publications include conference proceedings, monographs, data compilations, handbooks, sourcebooks, and special bibliographies.

TECHNOLOGY UTILIZATION PUBLICATIONS: Information on technology used by NASA that may be of particular interest in commercial and other non-aerospace applications. Publications include Tech Briefs, Technology Utilization Reports and Notes, and Technology Surveys.

Details on the availability of these publications may be obtained from:

SCIENTIFIC AND TECHNICAL INFORMATION DIVISION

NATIONAL AERONAUTICS AND SPACE ADMINISTRATION

Washington, D.C. 20546